ARISTOTLE UNIVERSITY OF THESSALONIKI
Interinstitutional Program of Postgraduate Studies in
PALAEONTOLOGY – GEOBIOLOGY

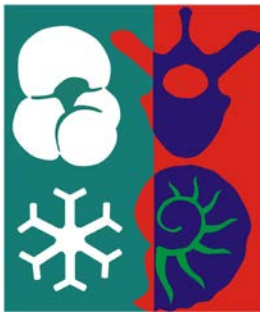

MARIA-SOFIA KAPIRI
Geologist

PALAEOCEANOGRAPHIC STUDY OF THE EPIDAURUS BASIN DURING THE LAST 1500 YEARS: AN ORGANIC BIOGEOCHEMICAL APPROACH

MASTER THESIS

DIRECTION: Micropalaeontology-Biostratigraphy
Directed by: National & Kapodistrian University of Athens

ATHENS
2023

Interinstitutional Program of Postgraduate Studies in PALAEONTOLOGY – GEOBIOLOGY

supported by:

Τμήμα Γεωλογίας ΑΠΘ
School of Geology AUTh

Τμήμα Βιολογίας ΑΠΘ
School of Biology AUTh

National and Kapodistrian University of Athens
Faculty of Geology and Geoenvironment

Τμήμα Γεωλογίας & Γεωπεριβάλλοντος ΕΚΠΑ

Faculty of Geology & Geoenvironment NKUA

Department of GEOLOGY

Τμήμα Γεωλογίας Παν/μίου Πατρών
Department of Geology, Patras Univ.

UNIVERSITY OF THE AEGEAN

Τμήμα Γεωγραφίας Παν/μίου Αιγαίου
Department of Geography, Aegean Univ.

MARIA-SOFIA KAPIRI
ΜΑΡΙΑ-ΣΟΦΙΑ ΚΑΠΙΡΗ
Πτυχιούχος Γεωλόγος

PALAEOCEANOGRAPHIC STUDY OF THE EPIDAURUS BASIN DURING THE LAST 1500 YEARS: AN ORGANIC BIOGEOCHEMICAL APPROACH

ΠΑΛΑΙΟΩΚΕΑΝΟΓΡΑΦΙΚΗ ΜΕΛΕΤΗ ΤΗΣ ΛΕΚΑΝΗΣ ΤΗΣ ΕΠΙΔΑΥΡΟΥ ΤΑ ΤΕΛΕΥΤΑΙΑ 1500 ΧΡΟΝΙΑ ΜΕΣΩ ΟΡΓΑΝΙΚΩΝ ΒΙΟΔΕΙΚΤΩΝ

Υποβλήθηκε στο ΔΠΜΣ Παλαιοντολογία-Γεωβιολογία

Ημερομηνία Προφορικής Εξέτασης: 13/10/2023
Oral Examination Date: 13/10/2023

Three-member Examining Board

Research Director HCMR Dr. Alexandra Gogou, Supervisor
Professor NKUA Maria Triantaphyllou, Member
Senior Researcher HCMR Dr. Constantine Parinos, Member

Τριμελής Εξεταστική Επιτροπή

Διευθύντρια Ερευνών ΕΛ.ΚΕ.Θ.Ε Δρ. Αλεξάνδρα Γώγου, Επιβλέπουσα
Καθηγήτρια ΕΚΠΑ Μαρία Τριανταφύλλου, Μέλος Τριμελούς Εξεταστικής Επιτροπής
Κύριος Ερευνητής ΕΛ.ΚΕ.Θ.Ε Δρ. Κωνσταντίνος Παρινός, Μέλος Τριμελούς Εξεταστικής Επιτροπής

Citation:
Kapiri M.S., 2023. – PALAEOCEANOGRAPHIC STUDY OF THE EPIDAURUS BASIN DURING THE LAST 1500 YEARS: AN ORGANIC BIOGEOCHEMICAL APPROACH. Master Thesis, Interinstitutional Program of Postgraduate Studies in Palaeontology-Geobiology. School of Geology, Aristotle University of Thessaloniki, 65 pp.

Table of Contents

Acknowledgements ix
Abstract x
Περίληψη xi
List of Figures xii
List of Tables xiii
1. INTRODUCTION 1
1.1. Palaeoclimate and climate variability in the Mediterranean Sea 1
1.2. Climate reconstructions derived from organic biogeochemical tools 3
1.2.1. *n*-alkanes and *n*-alkanols 4
1.2.2. *n*-alkan-1,15-diols and keto-ols 5
1.2.3. Isoprenoid derivatives 5
1.2.4. Long chain alkenones 6
1.2.5. Steroid alcohols 7
1.3. Physical oceanography of the Mediterranean and Aegean Sea 7
1.4. Purpose of the current master thesis 9
2. Study area 11
2.1. Region 11
2.2. Geology 13
3.Methodology 14
3.1. Sampling 14
3.2. Age model 14
3.3. Materials 15
3.4. Lipid extraction and separation 15
3.5. Identification and quantitative determination [GC-MS] 18
3.6. Lipid biomarkers and their application 18
3.6.1. Hydrocarbons and alcohols (*n*-alkanes and *n*-alkanols) and indices 19
3.6.2. Long-chain alkenones 21
3.6.3. Steroid alcohols 23
4. Result 24
4.1 SSTs 24
4.2. Marine input (alkenones and algal concentration) 24

4.3 Terrestrial input (*n*-alkanes and *n*-alcohols indices) 26
5. Discussion 31
6. Conclusions 38
6.1. Remarks 38
6.2. Current study and its future perspectives 39
7. References 41

Acknowledgements

The current master thesis was conducted at the Organic Chemistry Laboratory of the Institute of Oceanography of the Hellenic Centre for Marine Research (HCMR). This thesis was part of the Inter-Institutional Postgraduate Course "Palaeontology-Geobiology" in Aristotle University of Thessaloniki and in particular on the specialty of Micropalaeontology-Geobiology, which was held in the National and Kapodistrian University of Athens.

I would like to express my deepest appreciation to Prof. Maria Triantaphyllou, my supervisor, for the guidance and instruction with which she provided me throughout my master studies.

This endeavour would not have been possible without the valuable assistance and scientific contribution of my supervisor Dr. Alexandra Gogou, who provided me both the opportunity to have access to the laboratory and research facilities at the HCMR, as well as with the S25_1 core material and entrusted me with this master thesis and encouraged me in this academic path.

I am deeply indebted to my supervisor Dr. Constantine Parinos, who offered me invaluable feedback on the research, encouragement through the whole experimental process as well as provided me with great inputs and advice for my findings to be adequately interpreted.

I would like to express my gratitude to my internship's supervisor Dr. Belen Martrat, for her constant guidance, revisions, patience and support during the last and most crucial stages of my master thesis and for all the practical knowledge she imparted to me during my internship at IDAEA.

I benefited enormously from my supervirors' excellence both as teachers and as researchers and I consider myself to be extremely privileged to have been their student. The most important reason I want to thank them is because they taught me how to work efficiently and effectively as a scientist, how to properly cooperate with other researchers and they set the example of how a researcher should conduct themselves on both a personal and professional level. I hope and look forward to continuing doing research together.

In addition, I would like to extend my sincere thanks to Anastasia Christidi and Ester Skylaki for their guidance during the laboratory procedure and Elvira Plakidi and Stella Chourdaki for their assistance and advice throughout our collaboration at the HCMR.

Special thanks to Constantine Zakas, who was always there for discussions on anything that I was unsure of and for his accurate recommendations and modifications which were offered for this thesis.

Finally, I would like to express my gratitude towards my family and my friends, who supported and encouraged me during this master thesis.

Abstract

The current master thesis focuses on the palaeoenvironmental reconstruction in the Epidaurus Basin region which is located in the southwest Saronikos Gulf (eastern Mediterranean), over the past 1500 years. It addresses the interactions of the terrestrial and marine environments and the response modes of the marine environment in relation to the climatic changes observed in the area. For this purpose, the sedimentary record of the multicore S25_1 was analysed for selected biogeochemical markers and indices of terrestrial and marine origin, which convey a specific signal from the environment in which they were biosynthesised. The aforesaid biomarkers are lipid organic compounds, i.e. *n*-alkanes, *n*-alkanols, long chain alkenones and steroid alcohols that allow the reconstruction of the past, and specifically of parameters such as the sea surface temperature (SST), the hydrological regime, the paleo-productivity trends, the water mass circulation, the organic matter inputs and sources, the preservation *vs*. degradation of organic matte along with the stratification and oxygenation dynamics of the water column and the underlying sediment and the anthropogenic imprint that the region receives, mainly in the years of the industrial revolution (~ last 150 years). In the current thesis the age intervals that are analysed are 1) Dark Ages - DA (7^{th}-10^{th} centuries), with decreased SST compared to the rest of the dataset but concurrently with an upward trend, 2) Medieval Climate Anomaly – MCA (10^{th}-13^{th} centuries), which exhibited an upward trend in SST values, 3) Little Ice Age - LIA, which divides into two phases, namely the warming phase (13^{th}-16^{th} centuries) and cooling (16^{th}-19^{th} centuries) and 4) Industrial Period - IP (19^{th} century onwards), in which age interval the anthropogenic impact on the environment is observed through certain indicators and this century marked by a downward trend in SST values during the early 20^{th} century.

Keywords: Palaeoclimatology, Mediterranean, Biomarkers

Περίληψη

Η παρούσα διπλωματική εργασία έχει ως κύριο στόχο την ανασύσταση του παλαιοπεριβάλλοντος στη λεκάνη της Επιδαύρου, η οποία βρίσκεται στα νοτιοδυτικά του Σαρωνικού κόλπου (ανατολική Μεσόγειος), τα τελευταία 1500 χρόνια. Πιο αναλυτικά, ασχολείται με τον προσδιορισμό των αλληλεπιδράσεων χερσαίου και υδάτινου περιβάλλοντος και την απόκριση του θαλάσσιου περιβάλλοντος σε σχέση με τις κλιματολογικές αλλαγές που σημειώνονται στην περιοχή. Για την εμπεριστατωμένη μελέτη των προαναφερόμενων χαρακτηριστικών χρησιμοποιήθηκε το ίζημα του πυρήνα S25_1 και πιο συγκεκριμένα ορισμένοι βιογεωχημικοί δείκτες χερσαίας και θαλάσσιας προέλευσης, οι οποίοι μεταφέρουν ένα συγκεκριμένο σήμα από το περιβάλλον στο οποίο έγινε η βιοσύνθεσή τους. Οι βιοδείκτες αυτοί αποτελούν λιπιδικές οργανικές ενώσεις και συγκεκριμένα ανήκουν στις ομάδες *κ*-αλκάνια, *κ*-αλκανόλες, αλκενόνες και στεροειδείς αλκοόλες που επιτρέπουν την ανάπλαση των παρελθοντικών συνθηκών της εκάστοτε περιοχής και πιο συγκεκριμένα μέσω παραμέτρων όπως τη θερμοκρασία στην επιφάνεια της θάλασσας (SST), το υδρολογικό καθεστώς, τις τάσεις παλαιοπαραγωγικότητας, την κυκλοφορία των υδάτινων μαζών, τις εισροές και πηγές της οργανικής ύλης, τη διατήρηση έναντι της αποικοδόμησης της οργανικής ύλης μαζί με τη δυναμική της στρωμάτωσης και οξυγόνωσης της υδάτινης στήλης και του υποκείμενου ιζήματος, αλλά και του οικολογικού αποτυπώματος της ανθρώπινης δραστηριότητας που δέχεται η περιοχή, κυρίως τα χρόνια της βιομηχανικής επανάστασης (~ τα τελευταία 150 έτη). Στην παρούσα διατριβή τα ηλικιακά διαστήματα που αναλύονται είναι τα εξής: 1) η περίοδος των σκοτεινών χρόνων του Μεσαίωνα (Dark Ages - DA), (7^{ος}-10^{ος} αιώνας), που παρουσιάζονται μειωμένες τιμές SST σε σχέση με τα υπόλοιπα διαστήματα που αναλύονται αλλά με ταυτόχρονη αυξητική τάση, 2) η περίοδος κλιματικής ανωμαλίας του Μεσαίωνα (Medieval Climate Anomaly - MCA), (10^{ος}-13^{ος} αιώνας), το οποίο διάστημα παρουσίασε ανοδική τάση στις τιμές SST, 3) η μικρή Παγετώδης Περίοδος (Little Ice Age - LIA), η οποία χωρίζεται σε δύο φάσεις, τη θερμή φάση (13^{ος}-16^{ος} αιώνας) και την ψυχρή φάση (16^{ος}-19^{ος} αιώνας) και 4) τα χρόνια από την έναρξη της βιομηχανικής επανάστασης έως σήμερα (Industrial Period – IP), (19^{ος} αιώνας και μετά), κατά την οποία παρατηρείται σταδιακά η ανθρώπινη παρέμβαση στο περιβάλλον και στις αρχές του 20^{ου} αιώνα καταγράφονται μειωμένες τιμές SST.

Λέξεις κλειδιά: Παλαιοκλιματολογία, Μεσόγειος, Βιοδείκτες

List of Figures

Figure 1.: Geological and Historical Timeline (Gibbard et al., 2022).

Figure 2.: Major circulation features and gyres in the Aegean Sea. 1-Samothraki anticyclone, 2,3-North Aegean Sea gyres, c4-Central Aegean Sea cyclone, 5-Myrtoan Sea Cyclone, 6,7-Cretan Sea gyres (Velaoras et al., 2021).

Figure 3.: Time series of minimum (blue) and maximum (orange) average air temperatures of Meteo database, Isthmos Korinthou station 2008-2022.

Figure 4.: Bathymetric map of the multicore S25_1 (by using ArcMap 10.7.1).

Figure 5.: Information used to construct the age model, depth *vs*. CE ages (with 1σ error) for S25_1 core.

Figure 6.: The chemical reaction of an analyte Y:H with the formation of a TMS derivative (Moldoveanu & David, 2019).

Figure 7.: Simplified schematic representation of the analytical procedure.

Figure 8.: Paleo-dataset in Epidaurus Basin sediments over the last 1500 years. (A) CPI_{NA} and UCM and (B) ACL (C_{27-33} alkanes) and (C) TerNA and TerNOH (μg/g) and (D) Sea Surface Temperature (SST) (◦C) using alkenones and (E) Relative proportion of *n*-hexacosan-1-ol (*n*-C_{26}OH) to the sum of C_{26}OH plus *n*-C_{31} and HPA index and (F) ^{14}C age pointers with 1σ error.

Figure 9.: Paleo-dataset in Epidaurus Basin sediments over the last 1500 years. (A) Steroid alcohols (dinosterol, sitosterol, cholesterol, brassicasterol (ng/g) and (B) UCM/Tres and (C) Algal (μg/g) and alkenones (ng/g) concentration and (D) Sea Surface Temperature (SST) (◦C) using alkenones and (E) relative proportion of *n*-hexacosan-1-ol (*n*-C_{26}OH) to the sum of C_{26}OH plus *n*-C_{31} and HPA index and (F) ^{14}C age pointers with 1σ error.

Figure 10.: Paleo-dataset in Epidaurus Basin and Athos Basin sediments over the last 1500 years. (A) Sea Surface Temperature (SST) (◦C) using alkenones, (green for Epidaurus Basin and orange for Ahos Basin) and (B) relative proportion of *n*-hexacosan-1-ol (*n*-C_{26}OH) to the sum of C_{26}OH plus *n*-C_{31} and HPA index (grey for Epidaurus Basin and red for Athos Basin). The box in red shows the time interval within the ^{210}Pb range for M2 core (Athos Basin) (Gogou et al., 2016).

Figure 11.: (MedCLIVAR2k) Martrat et al., in prep.

List of Tables

Table 1.: Age model pointers for the investigated core S25_1.

Table 2.: Fractions and the solvents which are used in each sample.

Table 3.: Nomenclature of the steroid alcohols in the S25_1 core.

Table 4.: Statistical parameters of SST, TerNA, CPI_{NA}, Algal concentration and *n*-C_{26}OH values of the main age intervals of the last 1.5k.

1. INTRODUCTION

1.1. Palaeoclimate and climate variability in the Mediterranean Sea

The climatology discipline studies the climate as an aggregation over years of meteorological variations while oceanography focuses on the ocean as part of the hydrosphere, determining its geological, chemical, physical and biological conditions. Both words preceded by the prefix paleo (palaios~ancient) introduce the approach from history, the past. The instrumental measurements are a legacy of exceptional value, though they cover from few decades to centuries in the best of cases. It is necessary to compare and complete them with the data provided by indirect climatic sensors (proxies), which are contained in archives such as historical documents, archaeological strata, tree growth rings, ice cores, speleothems in caves, corals, lacustrine and marine sediments, among others (Dobrovolný et al., 2010; Drăguşin et al., 2014; Felis et al., 2000; Gogou et al., 2016; Zanchetta et al., 2012). These contain information and sensors of past environmental signals (temperature, precipitation and other variables).

There are ongoing efforts to revise the Mediterranean paleoclimate archives and improve the spatial coverage to facilitate evaluation of contrast/see-saws from the western to the eastern part, the latter currently poorly represented within latest compilations (Consortium, 2017; Hernández et al., 2020; Konecky et al., 2020). Traditionally, many of the detailed climate series reconstructions have been based on terrestrial archives. High-resolution marine archives have received less attention, considering the highly relevant fraction that the ocean represents (2/3 of the Earth) and its fundamental role in the environment. In this context, marine sediments are used to reconstruct the oceanographic and environmental conditions of each region and specific period of time (Incarbona et al., 2016).

Within Koppen's climate classification, the current Mediterranean climate is transitional between the temperate and tropical zones, with dry and hot summers and mild, rainy winters affected by westerly circulation (Mahairas & Balafoutis, 1997; Peel et al., 2007). Following the Martonne's classification for the hydroclimate of the Mediterranean, the region is spatially confined between the warm temperate fully humid climate from the north and the arid climate from the desert in the south. Furthermore, a wide variety of local and occasional climatic phenomena result in land-sea interactions/connections, from the northwestern transitional continental regimes to the southeastern subtropical climates (Lolis et al., 2002). Specifically for the eastern Mediterranean and the Aegean areas, winds blowing during the summer season promote mild winters, cool summers, low to moderate precipitation, long summer drought and high frequency of strong wind currents (Mahairas & Balafoutis, 1997).

The Mediterranean climate variability changed during the Holocene (i.e., the present interglacial period, from 11.7k to present (Fig. 1); (Gibbard et al., 2022), following three phases. First, from 11.7 to 8.2k (Greenlandian), the final part of the deglaciation, when the seasonal cycle of the northern hemisphere increased, causing the African monsoons to shift to northern areas influencing the eastern Mediterranean climate (e.g., Triantaphyllou et al., (2009)). The result was perturbations to thermohaline circulation and massive freshwater

discharge through precipitation levels and river runoff. The freshwater-driven stratification caused seafloor anoxia below a depth of approximately 1800 m (Incarbona et al., 2019), as a result of both a failure of deep water formation and enhanced productivity in the euphotic zone (Rohling, 1994; Rohling et al., 2015).

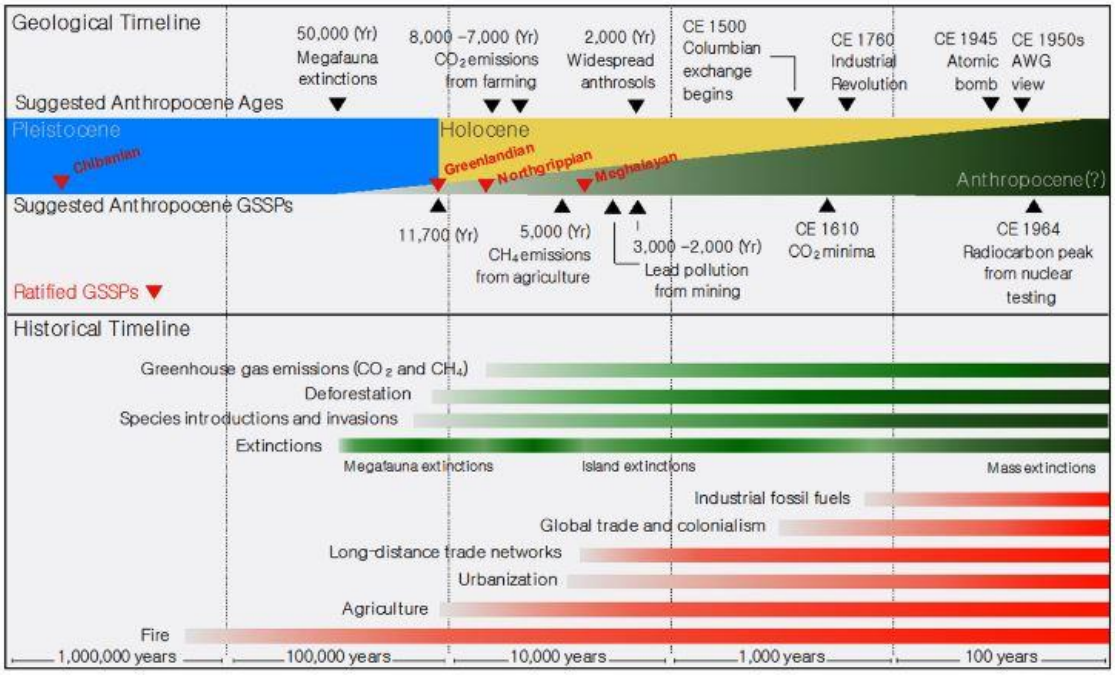

Figure 1.: Geological and Historical Timeline (Gibbard et al., 2022).

Second, from 8.2k to 4.2k (Northgrippian), which proves the existence of sudden climate oscillations that can occur even over a little period of time and affect specific areas or can develop into a large-scale phenomenon. A representative example of the aforesaid condition is sapropel S1 (deposited ca. from 10.8k to 6.1k), which in some areas shows an interruption during the 8.2k cold period, differing in others (Walker et al., 2012).

Third, from 4.2k to present (Meghalayan), which includes the period studied here (past 1.5k) and presents several events that point to the Mediterranean area as a region sensitive to complex environmental and oceanographic climate changes. For instance, reconstructed surface temperature changes over this period in the northern Iberian peninsula, using high-resolution stable carbon isotope records of stalagmites from three limestone caves, identified different time intervals as follows (Martín-Chivelet et al., 2011): (a) the Roman Warm Period (RWP) as a warm period (-550-300 years before the common era, BCE); (b) the Dark Ages Cold Period, a notably cold interval (lasting from 300-600 years of the common era, CE), with a thermal minimum at approximately 450 y CE; (c) the Mediaeval Climate Anomaly (MCA), with generally warm conditions from 600-1250 y CE, namely the, are recorded and two cooler events at 700 and 1100 y CE respectively; (d) the Little Ice Age (LIA), with lower temperatures during the subsequent period (1250-1850 y CE), including cooling extremes at 1350-1450 y CE, 1600-1650 y CE and finally (e) the Modern Warming, the past 0.150k, from 1850 y CE to present, characterised by rapid but non-linear warming (Martín-Chivelet et al., 2011; Roberts et al., 2012).

Studies with high-resolution records from lake and marine archives and tree rings from Iberia and Morocco indicate lower water levels and higher salinities during the MCA and wetter conditions during the LIA (Esper et al., 2007; Roberts et al., 2012). On the contrary, evidence from lake and speleothem indicators from Turkey show a converse pattern with wet conditions during the MCA and dry conditions during the LIA for the eastern Mediterranean (Roberts et al., 2012). Therefore, a dissimilar pattern between eastern and western climates is suggested, which seems to be taking place during the past millennium in the Mediterranean region. However, more information is needed from the eastern Mediterranean (Cook et al., 2016; Roberts et al., 2012) and the present study aims to help in understanding the climate dynamics in the region.

The most important large-scale atmospheric modes of climate variability in the Northern Hemisphere with implications to the climate distribution over the Mediterranean Sea are the North Atlantic Oscillation (NAO) and the AMO (Atlantic Multidecadal Oscillation) (Hernández et al., 2020). Both of these indices explain significant climate phenomena on the weather patterns and variability in the Mediterranean region. The NAO represents a north-south seesaw pattern of atmospheric pressure between the Icelandic Low and the Azores High (Hurrell et al., 2003). The AMO is a natural climate cycle characterised by fluctuations in the sea surface temperatures of the North Atlantic Ocean and can have a profound influence on temperature and precipitation patterns in the Mediterranean region, characterised by a cycle of 70 years (Marullo et al., 2011).

1.2. Climate reconstructions derived from organic biogeochemical tools

It should be mentioned that records from instrumental measurements and techniques can offer valuable information for determining past climate changes and fluctuations. Nonetheless, time series of measured environmental parameters are not always able to capture short-term processes, non-analogue situations and rare and local events, since they are most often temporally inhomogeneous and spatially very inconsistent (Versteegh, 2005). Hence, instrumental records fail to capture the overall view of climate variability and oscillations (Jones et al., 2001), and marine records and different biomarkers measured in their strata help in embracing the whole environmental evolution.

Biomarkers are the organic compounds which are produced by all organisms both in the terrestrial and in the marine environment. Their fundamental chemical composition consists of carbon and hydrogen atoms. Additionally, the aforesaid organic molecules are preserved in rocks, soil and sediments and in rocks which correlate to petroleum molecules (Eglinton & Hamilton, 1967; Tyson, 2006). Some organic compounds are resistant to environmental conditions, while other organic molecules subject to changes due to environmental stress and degradation have also a recognizable structure. This fact leads to the provision of information about the process they have undergone and organic molecules can be considered as chemical fossils (Rosell-Melé & McClymont, 2007). In summary, the determination of biomarkers provides information about the origin of the organic matter, i.e. terrestrial or aquatic, the diagenetic conditions that the respective sediment underwent and the paleoenvironmental

conditions during their biosynthesis (Brocks & Grice, 2011; Luo et al., 2018). It should also be mentioned that as the sediment depth and water column increase, the absolute amounts of organic compounds decrease and this constitutes the outcome of diagenesis (Rosell-Melé & McClymont, 2007).

Lipid biomarkers constitute one of the most important classes of molecular markers. These compounds are produced by organisms, are insoluble in water and soluble in non-polar solvents that dissolve fats, particularly *n*-hexane, dichloromethane and toluene (Luo et al., 2018). This category includes substances such as fatty acids, alcohols, hydrocarbons, glycerol esters and ethers (Luo et al., 2018).

Hence, biomarker proxies can be employed to gain quantitative and qualitative measurements and results for palaeoceanographic and climatic parameters, and area useful tool for the reconstruction of past sea surface temperatures (SSTs), land-ocean interactions, marine productivity etc. The previously mentioned results can be associated altogether to the study of biogeochemical cycles and climate change.

1.2.1. *n*-alkanes and *n*-alkanols

Aliphatic hydrocarbons (AHs) are amid the most ubiquitous organic compounds in various environments, such as coastal and pelagic sites (Dachs & Méjanelle, 2010; Hasanuzzaman et al., 2007). The previously mentioned compounds, for instance *n*-alkanes, isoalkanes, cycloalkanes, terpenes, hopanes, and steranes, are derived from both biogenic sources, such as terrestrial plant waxes, marine phytoplankton and bacteria and anthropogenic ones (Duan Fengkui et al., 2010; Rushdi et al., 2006), and are the major constituents of petroleum products, crude oil and refined fossil fuel (Wang et al., 1999). AHs, mainly *n*-alkanes, are introduced to the marine environment via both atmospheric, dry and wet deposition, gas exchange across the air-water interface and aquatic pathways, i.e. direct discharges, continental run-offs, off-shelf export) the relative importance of which largely depends on the geographical setting of a given area (Parinos et al., 2013). Pertaining to anthropogenic sources, AHs enter marine environments through atmospheric dust, runoff, spillages, industrial and sewage effluents, shipping activities, and natural oil seepage (Appolinario et al., 2020; Huguet et al., 2019; Rushdi et al., 2018), as well as by organic matter biodegradation (Rushdi et al., 2018) a fact which results in the formation and release of hazardous organic pollutants (Al-Khion et al., 2021). The *n*-alkanes constitute the simplest hydrocarbons and are relatively inert under oxidising and reducing conditions. Their general chemical formula is C_nH_{2n+2}.

The *n*-alkanols belong to the category of alcohols with a straight carbon chain. The aliphatic alcohols can be regarded as derivatives of alkanes, in which one or more hydrogen atoms have been replaced by hydroxyl groups [−OH] with a general chemical formula of $C_nH2_{n+1}OH$. Homologues of long chain *n*-alkanols, as well as the *n*-alkanes, typically appear in terrestrial and marine sediments (Cranwell, 1972; Huang et al., 2000). Further, high molecular weight *n*-alkanes and *n*-alkanols are the major components of epicuticular plant waxes (Eglinton &

Hamilton, 1967), and have been often used as proxies of allochthonous natural (terrestrial) inputs into the marine environment (Gogou et al., 2007; Ohkouchi et al., 1997).

n-alkanes and *n*-alkanols, have been previously used as proxies in palaeoclimatology to reconstruct past climate and to estimate past climate variations, environmental conditions and ecological changes in the eastern Mediterranean and Aegean Sea region (Gogou et al., 2007; Kouli et al., 2012, Parinos et al., 2013).

1.2.2. *n*-alkan-1,15-diols and keto-ols

Diols are organic aliphatic chemical compounds containing two hydroxyl groups (−OH groups). Especially for long-chain C_{30} *n*-alkan-1,15-diols, they have been found both in marine and freshwater settings (Pedrosa-Pàmies et al., 2015, 2018, 2019; Rampen et al., 2012; Versteegh et al., 2000), notwithstanding their exact biological sources are still under investigation. The known biological precursors of long-chain diols are marine nannoplankton of the class Eustigmatophyta, first discovered in particular in the *Nannochloropsis spp.* microalgae (Gelin et al., 1997; Volkman, 1986).

Ketols are organic compounds, which have both an alcohol (CH_2OH) and a keto (=CO). The present thesis is taking into account the C_{30} 1,15-keto-ol, which seemingly constitutes an oxidation product (Menzel et al., 2003) of the corresponding C_{30} diols (C_{30} 1,15-diol) (Rampen et al., 2012; Volkman, 1986; Volkman et al., 1999) formed during settling of particles in the water column or in the sediment and/or, as has been recently proposed by (Versteegh & Lipp, 2019), by yet uncharacterized source species. Nonetheless, the long-chain diols have been identified in Proboscia diatoms as well (Rampen et al., 2008; Rodrigo-Gámiz et al., 2013). Finally, the aforementioned compounds used as biomarkers in the studies of past climate conditions, particularly in the analysis of sedimentary records such as lake sediments and marine cores.

1.2.3. Isoprenoid derivatives

Loliolide (1,3-dihydroxy-3,5,5-trimethylcyclohexylidene-4-acetic acid lactone) constitutes a monoterpene (Percot et al., 2009), which is a chemical class of terpenes, consisting of two isoprene units, has the molecular formula $C_{10}H_{16}$ and belongs to the secondary metabolites produced by organisms, for instance plants and fungi.

Pertaining to the origin of loliolides it is suggested that loliolide/isololiolide is an anoxic degradation (Menzel et al., 2003) or a photo-oxidation product of algal carotenoids, such as fucoxanthin, the major carotenoid in diatoms, as well as in dinoflagellates and haptophytes (Klok et al., 1984; Menzel et al., 2003) and zeaxanthin (Isoe et al., 1972; Repeta, 1989). As such, loliolides are utilised as biomarkers for photo-oxidative alterations of phytoplankton in sediments (Klok et al., 1984).

Diatom blooms are characteristic of highly productive areas, like upwelling regions where cold and nutrient-rich waters reach the euphotic zone. Consequently, the rapid increment in loliolide/isololiolide accumulation rates reveals a quick change in nutrient-rich conditions (Menzel et al., 2003).

Moreover, as it is clear by the above, during oxic deposition conditions, the formation of loliolide from fucoxanthin is impossible, since loliolide is a photosynthetic product under hypoxic to anoxic conditions. Therefore, the aforesaid proxies are abundant in sapropelic layers and in the εastern Mediterranean. Finally, the abundance and distribution of these compounds in sediments along with other organic compounds can be used to reconstruct past environmental conditions such as primary productivity and nutrient availability.

1.2.4. Long chain alkenones

Alkenones belong to the homologous series of unsaturated methyl- and ethyl-ketones and they have characteristic long carbon chain homologues consisting of 37 to 39 carbon atoms, occurring in marine particles and sediments. They are biosynthesized by a very specific group of the order of Haptophytes, also known as Prymnesiophytes, the coccolithophores and specifically by the species *Emiliania huxlei* and *Gephyrocapsa oceanica* (Sawada et al., 1996). Long-chain alkenones reflect the productivity of haptophyte algal species of the Prymnesiophyte class. *Emiliania huxlei* species, in particular, is the most abundant and widespread coccolithophore in the oceans and is considered the dominant producer of alkenones in the modern environment. On the other hand, *Gephyrocapsa oceanica* constitutes an important contributor mainly in warmer tropical and subtropical regions (Sikes et al., 1997; Volkman et al., 1995).

Several measurements of alkenones in the water column have shown that their maximum production is located on the surface layer of the sea (Herbert, 2003). Generally, the time of maximum abundance of *E. huxleyi* and/or *G. oceanica* and the maximum flux of alkenones into sediment traps coincides with the dominant period of phytoplankton blooming. Hence, production positively peaks in spring months in most subtropical and mid-latitude locations (Broerse et al., 2000; Cortés et al., 2001; Harada et al., 2001; Sprengel et al., 2000). Furthermore, despite the fact that the alkenones are the product of calcareous algae, they are also able to survive in sediments where carbonate has dissolved.

In general, another characteristic of alkenones is their resistance to chemical degradation and consequently their preservation in marine sediments. Their remarkable durability is due to the presence of double bonds in their molecules. While usually double bonds are sensitive to degradation processes, in alkenones they have an unusual trans geometric isomerism (they cannot be rotated), which does not allow their coupling and makes them particularly stable/recalcitrant to diagenesis in the water column and within the sediment (Herbert, 2003) and resistant to degradation by bacteria. The first reported occurrence of alkenones was identified in Miocene through Pleistocene age marine sediments on the Walvis Ridge (Boon et al., 1978).

In addition to the biogeochemical information, which is extracted from the study of the aforementioned long-chain unsaturated ketones, the correlation between the abundance of alkenones and the temperature of the seawater, where their biological precursors, the coccolithophores, grow, has been confirmed. In order to allow for a direct comparison between alkenone unsaturation and water (growth) temperature (Brassell et al., 1986), the ketone unsaturation index U_{37}^{k} was introduced. This index will be further analysed in the following chapters. In the Aegean Sea area, there have been studies such as that of Gogou et al. (2007) and Triantaphyllou et al. (2009) using alkenones for the reconstruction of past SST.

1.2.5. Steroid alcohols

Steroid alcohols constitute essential lipids in eukaryotic membranes controlling the membrane permeability and rigidity (Volkman, 1986). Moreover, their broad diversity, biosynthetic specificity and good stability toward diagenetic reworking in marine sediments render them adequate indicators for marine particulate and sedimentary organic matter (Hudson et al., 2001; Nash et al., 2005; Volkman, 2005) and environmental changes (Mouradian et al., 2007), e.g. the sum of algal concentrations, in both the modern and ancient ocean.

An amble variety of functionalized steroids was identified in recent sediments and is categorised by the number and position of double bonds, hydroxy-, oxo- and alkyl groups, and other complex substituents. They can be diagnostic for an array of taxonomic groups, in particular algae (Volkman, 2003). By the same token, marine sterols are main constituents of several marine phytoplankton groups (Menzel et al., 2003; Volkman et al., 1999). For instance, brassicasterol (28$\Delta^{5,22E}$, 24-methylcholesta-5,22-dien-3β-ol) is the major sterol in many diatoms, yet it also occurs in some prymnesiophytes, principally *Emiliania huxleyi* and in general is considered a strict phytosterol, i.e. it cannot be biosynthesized by zooplankton (Cavagna et al., 2013). Dinosterol (30Δ^{22E}, 4α,23,24-trimethyl-5α(H)cholest-22(E)-en-εβ-ol) constitutes a major compound in dinoflagellates (dinocyst) and is commonly used in palaeoceanography as source-specific biomarkers of this algal species (Mouradian et al., 2007; Volkman, 1986; Volkman et al., 1999). Cholesterol (27Δ^{5}, cholest-5-en-3β-ol) is produced by some algae (Cavagna et al., 2013; Volkman, 1986) and it is commonly considered a biomarker for consumer organisms and a proxy for zooplanktonic herbivory (Grice et al., 1998). Finally, β-Sitosterol (C29Δ^{5}, 24-ethylcholest-5-en-3β-ol) can be found in both terrestrial and marine environments (Volkman, 1986).

1.3. Physical oceanography of the Mediterranean and Aegean Sea

The Mediterranean is a semi-enclosed sea adjacent to the Atlantic Ocean. The main feature of the Mediterranean is the intense evaporation in relation to precipitation. As a corollary of the above factor, high temperatures and high salinity values prevail, especially in the eastern Mediterranean. The low-salinity Atlantic Water (AW) penetrates the surface, low-density waters of the Mediterranean and is transformed into high-salinity and dense Mediterranean

water, which flows from the lower aquatic layers of the Strait of Gibraltar (Theocharis et al., 1993). The basic characteristics of the AW weaken as it heads towards the eastern Mediterranean, due to water mixing and evaporation. As a result, the waters of the western Mediterranean are colder than those of the eastern Mediterranean. The creation of intermediate and deep waters occurs in exclusive areas within the Mediterranean basin (Robinson et al., 1992).

The marine environment of the eastern Mediterranean is controlled by the local climate, the inflow of waters from the main rivers that flow through southeastern Europe and the Nile, as well as the seasonal fluctuations of surface waters flowing into the Aegean Sea from the Black Sea. The eastern Mediterranean area is an oligotrophic area mainly due to the inflow of nutrient-poor, surface water of the Atlantic and the corresponding outflow of relatively nutrient-enriched intermediate waters through the Sicily Strait (Tselepides et al., 2000). In this oligotrophic environment with well-oxygenated waters, the depth of life of the foraminiferal assemblages is limited by the availability of food and the populations show low values of concentrations and low variety of species, with the predominance of epifaunal forms (Triantaphyllou & Dimiza, 2012).

The Aegean Sea is located in the transitional climate zone between temperate and semi-arid climates. It has a small size, covering an area of 240000 km^2, but is notwithstanding characterised by complex bathymetry (Triantaphyllou et al., 2016). The Aegean Sea is surrounded by Greece and Turkey, it communicates with the Black Sea, through the Dardanelles strait and with the Mediterranean Sea and the Levantine Basin, through the Cretan straits. The thermal circulation of the Aegean Sea constitutes a quite complex process (Fig. 2.). The Aegean is characterised by high water densities in the deep basins, with the densest waters found in the deep basins of the north Aegean Sea. The circulation of the Aegean Sea is mainly cyclonic (Velaoras et al., 2021) with warm saline waters, originating from the Levantine basin and entering the Aegean from the eastern straits of Crete.

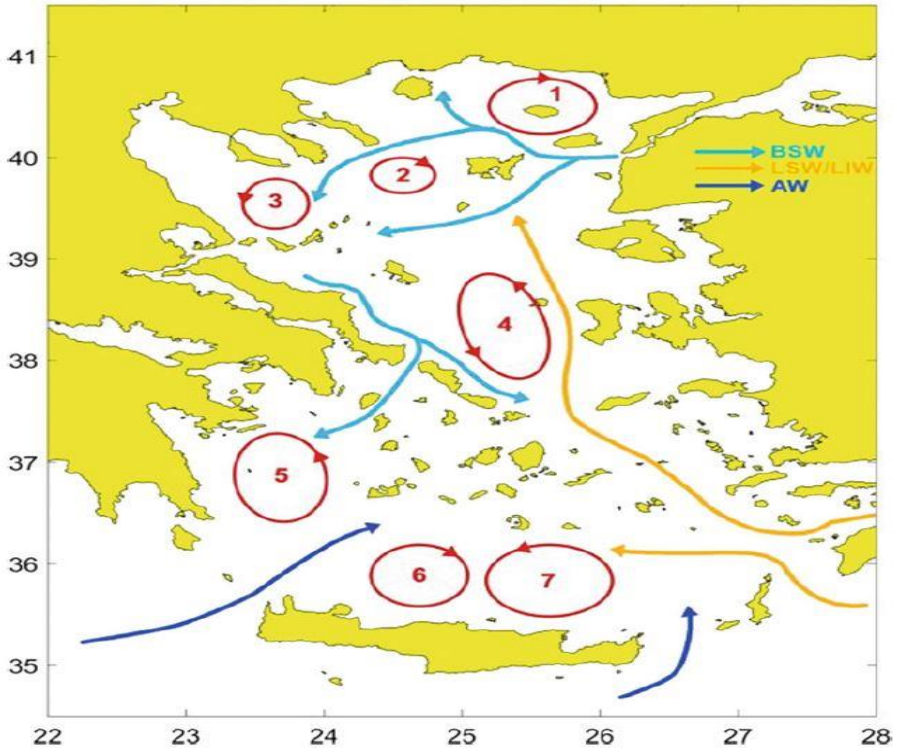

Figure 2.: Major circulation features and gyres in the Aegean Sea. 1-Samothraki anticyclone, 2,3-North Aegean Sea gyres, 4-Central Aegean Sea cyclone, 5-Myrtoan Sea Cyclone, 6,7-Cretan Sea gyres (after Velaoras et al., 2021).

In terms of productivity, the Aegean Sea is quite an oligotrophic environment, with limited growth of phytoplankton and zooplankton (Michelakaki & Kitsiou, 2005). The north Aegean is characterised by an increased concentration of nutrients compared to the South Aegean, due to the waters of the Black Sea, which enter the Aegean through the Dardanelles Straits. The above characteristics are related to the topography of the area, i.e. the extensive continental shelf, as well as the inflow of water from rivers of Greece and Turkey. Finally, the increased concentration of nutrients is also related to the intense hydrological complexity that prevails in the northern Aegean region (Zanetos & Papathanassiou, 2005). The area studied in this thesis is the Epidaurus Basin, which is in the Saronikos Gulf, which is adjacent to the Aegean Sea.

1.4. Purpose of the current master thesis

The present master thesis focuses on the palaeoenvironmental reconstruction in the Epidaurus Basin during the last 1500 years, the determination of the interactions of the terrestrial and marine environments through marine and terrestrially-derived biogeochemical markers and their diagnostic indices, the response modes of the marine environment in relation to the climatic changes observed in the area and the estimation of the anthropogenic pressures that the region receives, mainly in the years of the industrial revolution. The endeavour of reconstructing the palaeoenvironmental conditions in the Mediterranean region is one of the largest ongoing investigations and the findings of the Epidaurus multicore

will contribute both to the establishment of a denser data network for the northeastern Mediterranean region and to estimate the sensitivities and peculiarities of the Mediterranean climate mode. The age intervals that analysed were the Dark Ages (DA), the Medieval Climate Anomaly (MCA), the Little Ice Age (LIA) and the years from the start of the industrial revolution to the present day (IP). The indicators used were mainly related to the Sea Surface Temperature (SST), the terrestrial inputs and the consequent nutrient supply to the marine environment, the marine productivity, the water column stratification *vs*. mixing processes, shaping the oxygenation levels of the seabed along with the preservation *vs*. degradation of organic matter of both marine and terrestrial origin. The analysis of the results showed several palaeoenvironmental trends for the Saronikos Gulf, central Aegean region.

2. Study area

2.1. Region

The Saronikos Gulf (Fig 3) constitutes a semi-enclosed embayment on the western part of the Aegean Sea (eastern Mediterranean Sea) and is situated between the peninsulas of Attica and Argolis. It covers approximately 2800 km^2 and has a maximum depth of approximately ~ 400 m west of the Methana volcano, in the south part which is called Epidaurus Basin, while in general it is characterised by a complex bathymetry (Triantaphyllou et al., 2018; Zervoudaki et al., 2022). The western part, located west of the islands of Aegina and Salamis, consists of the greatest depths, while the inner gulf, located in the northern area of the eastern part, is relatively flat, with an average depth of about 90 m (Kontoyiannis, 2010). The outer gulf, in the SE, is connected to the Aegean Sea and has depths that gradually decrease towards the inner gulf and the coasts of Attica from about 200 m to 100 m (e.g., Triantaphyllou et al., (2018)).

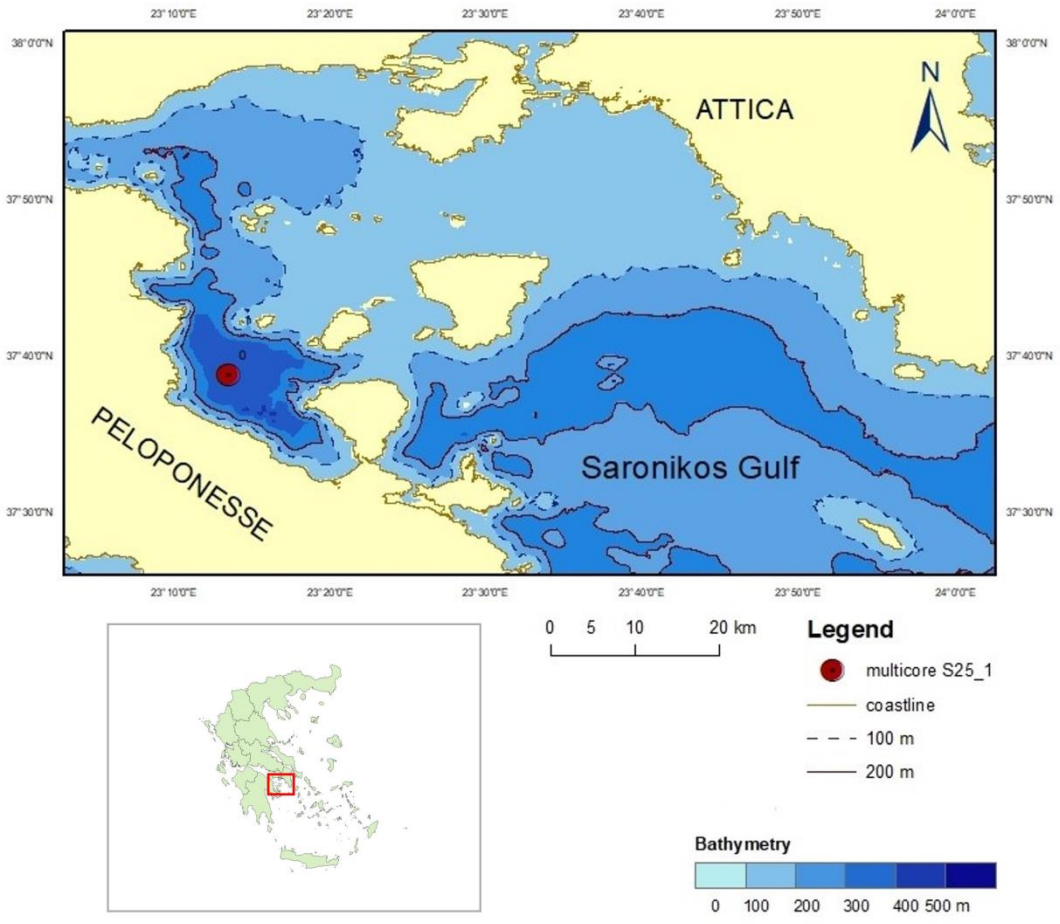

Figure 3.: Bathymetric map of the multicore S25_1 (by using ArcMap 10.7.1).

Specifically for the circulation of the Saronikos Gulf, a distinct two-layer structure in the period from late spring to summer up until late fall is clearly noticeable, whereas it is basically barotropic during the rest of the months, namely December to March (Kontoyiannis, 2010). Density contrasts between local water masses and masses that originate from the open sea in the south along with local thermohaline forcing, namely winter cold water subduction and different responses to atmospheric heating of shallow compared to deep areas of the Gulf, are associated with robust seasonal flow structures, which are modified by local winds. The aforementioned modifications are more pronounced at depths above the thermocline in the stratification period. More particularly, an anticyclonic flow prevails in the upper 100 m of the water column during winter and early spring and cyclonic and an anticyclonic flow occurs in the upper 0 to 40 m and deeper approximately 60 to 100 m water layers, respectively through late spring to early summer (Kontoyiannis, 2010).

Particularly for the Epidaurus Basin, it is characterised by a slow exchange of water masses. It is relatively isolated from lateral water exchanges at depths greater than 100 m (Friligos, 1983), which is the average depth of the Saronic Gulf (Zervoudaki et al., 2022). Consequently, deeper areas may be oxygenated by submergence of newly formed dense water masses during winter. Furthermore, the seasonality in the area is quite high (Fig. 4), thus there is the potential for cold water transmission to the shallower areas of the gulf due to atmospheric cooling that occurs in winter and the lateral transfer of these sinking water masses (Kontoyiannis et al., 2023).

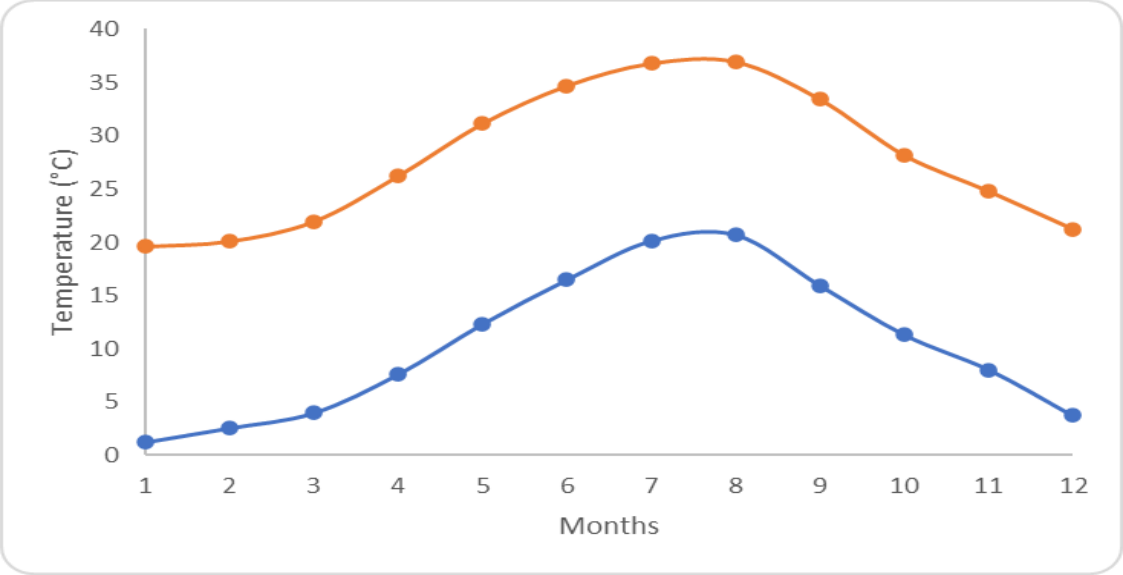

Figure 4.: Time series of minimum (blue) and maximum (orange) average air temperatures of Meteo database, Isthmos Korinthou station 2008-2022.

2.2. Geology

The geology of the Argolis is characterised as quite complex, since a great variety of formations, units and phases are observed, while the abrupt change of phases is sometimes explained by tectonic contact and occasionally by abrupt transition into another geological unit (Matiatos, 2010).

The wider area of the Epidaurus Basin consists mainly of the Pelagonian Zone. This zone consists of metamorphic and non-metamorphic rocks, mainly neritic carbonate sediments and in general constitutes a neritic platform. More specifically, flysch, boeotian flysch, limestones of the Late Cretaceous and Jurassic-Triassic limestones of the Trapezona's formation are exhibited (Matiatos, 2010). The formation of Trapezona is a platform dating back to Late Jurassic which had been getting deeper until the Early Cretaceous (previously known as Neocomian) (Matiatos, 2010).

The transition from neritic to pelagic sedimentation occurs earlier in the east section, where it begins in the Middle Liassic (Late Jurassic), than in the west section, where it begins after the Toarcian, which results in a westward migration of the platform margin. The lateral phase changes observed in the Triassic deposits indicate local changes in sedimentological conditions and anomalous topography of the basin floor. Moreover, in the wider area, rocks from the Upper Paleozoic and Permotriassic formations that are unclassified, and shales that belong to the lower ophiolitic unit of the area can be observed. Based on lithological petrographic and structural analyses of the ophiolitic complex in the northern Argolis, 3 ophiolite units were defined (Tzanis et al., 2018) .

In particular, the lower ophiolitic unit consists of an ophiolitic sedimentary melange that was deposited before the end of the Late Jurassic. Its base consists of red siliceous siltstones and keratolites with radiolarians, which is upwards characterised by the presence of ophiolitic mudstones and clastic limestone sediments (Tzanis et al., 2018). Alluvial deposits and Quaternary calc-alkaline volcanic rocks, particularly andesites to dacites are observed as well (Tzanis et al., 2018). Ultimately, regarding the marine area, fine sediments such as muds are established in the deeper sites of the Saronikos Gulf, while sands are mapped in the central region and near coastal areas (Foutrakis & Anastasakis, 2020).

Another important fact that should be pointed out is that the Saronikos Gulf is located in the NW part of the Hellenic volcanic arc and represents the western end of it and is more particularly situated between the Pliocene volcano of Aegina and the Pleistocene volcanoes of Methana and Sousaki (Drakatos et al., 2005). The volcanic arc of the South Aegean (Aegean Volcanic Arc) is composed of submarine, terrestrial and island volcanoes, from the Saronic Gulf to the submerged area of Kos-Nisyros. The structure is formed by upwardly moving magma, which originates mainly from the melting of the rocks of the subducting African tectonic plate beneath the Eurasian plate, when it reaches depths greater than 100 km (Papanikolaou & Sideris, 2014).

3.Methodology

3.1. Sampling

The multicore S25_1 was retrieved in one tube on 29/09/2014 from the Epidaurus Basin, Greece (Saronikos Gulf, 37.6451, 23.2237) onboard the R/V 'Aegaeo' during the WFD (Water Framework Directive) cruise at a water depth of 402 m (Fig. 3). The 46.5-cm long core was sampled continuously at a sampling step of 0.5 cm.

3.2. Age model

An age-depth model has been constructed by accelerator mass spectrometry (AMS) ^{14}C dates (Table 1) Specifically, three accelerator mass spectrometry (AMS) ^{14}C dates were performed at the laboratories of Beta Analytic (USA) on cleaned hand-picked planktonic foraminifera (mostly *Globigerinoides ruber*). ^{14}C ages were converted into calibrated ages using the Calib v.7.02 software (Reimer et al., 2013) and the MARINE13 calibration dataset, using the local marine reservoir age of 73 ± 61 years (Facorellis & Vardala-Theodorou, 2015). The age model is based on linear interpolation between the ^{14}C dates and presented in Fig. 5.

Table 1.: Age model pointers for the investigated core S25_1.

Depth (cm)	Material	^{14}C (BP)	cal year CE, 1σ	Mean age (CE)
11	planktonic forams	270 ± 30 [a]		1730
19.25	planktonic forams	880 ± 30	1447-1573	1510
46	planktonic forams	1870 ± 30	543-678	610.5

[a] Result out of calibration range.

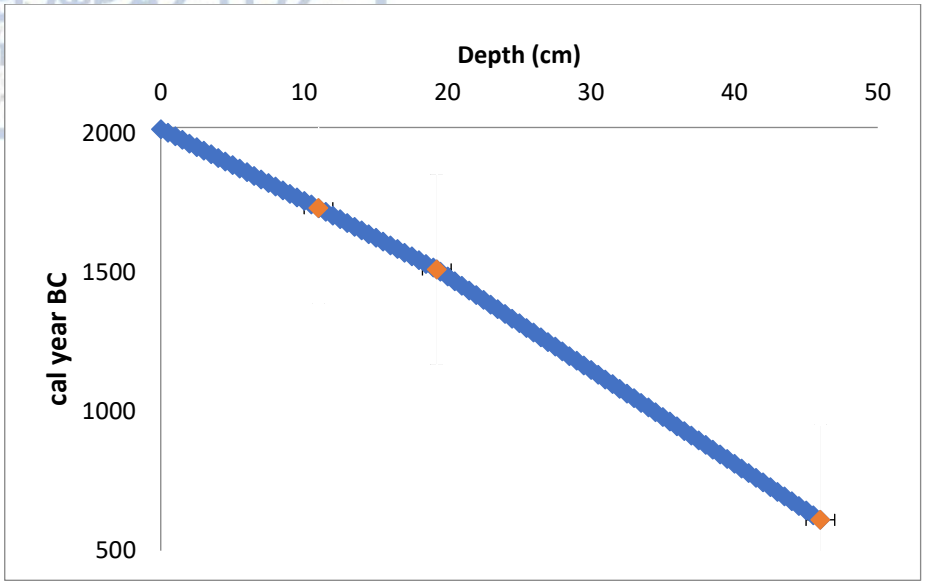

Figure 5.: Information used to construct the age model, depth *vs.* CE ages (with 1σ error) for S25_1 core.

3.3. Materials

The utilised solvents were of high purity grade (Merck, Suprasolv grade) and silica gel with 230-400 mesh particle size and were procured from Merck (Darmstadt, Germany). All laboratory glassware were combusted at 450°C for 6 hours before they were utilised in the laboratory process. Equipment which could not be purified by high temperatures, e.g. syringes, stopcock of glass columns were cleaned using organic solvents. Procedural blanks run in parallel to the samples where free of any contamination in all cases.

3.4. Lipid extraction and separation

The sediments before the analytical process were freeze-dried and thenceforth a mortar was utilised to grind the samples into a fine powder. From the integrated material 2 gr to 4 gr of each sample was collected for the extraction process and then placed into test tubes, depending on the total organic carbon concentration. Further, the samples were spiked with the following internal standards, for quantitative determinations during the gas chromatography step.

- A [$^{2}H_{50}$] *n*-tetracosane for aliphatic hydrocarbons
- *n*-$C_{21}D_{43}O$/5α-androstan-3β-ol for *n*-alkanols and steroid alcohols respectively
- *n*-$C_{36}H_{74}$ (surrogate standard for the long chain alkenones fraction)

Following the initial stage, the samples were solvent extracted according to the analytical protocol proposed by Gogou et al. (2007) (Table 2, Fig. 7). A 4:1 (*v/v*) mixture of CH_2Cl_2 and MeOH was employed. Initially, 20mL of solvent were added to the test tube of each sample,

which was left for 15 min in a sonicator at 25°C and after that stage the samples were left inert for 10 min before the next step. The solution was then transferred with a glass pipette into a conical flask and underwent infiltration using glass wool and Na_2SO_4 as a desiccant and the final mixture was collected into a pear-shaped glass flask. The extraction scheme was repeated three times while finally the Na_2SO_4 is washed with CH_2Cl_2. Combined extracts were then concentrated in a rotary evaporator. Each sample was transferred to a 1.5 mL vial under nitrogen flow with CH_2Cl_2 as transfer solvent, always leaving a sufficient amount of solvent (200-300 μL) so that it was not concentrated to dryness. Before column chromatography the sample's solvent was changed to *n*-hexane under a gentle nitrogen stream.

The second stage of the laboratory analysis includes the silica activation step, the column preparation, the sample placement and the fractions' collection and the concentration of the final aliquot and its collection. Regarding the fourth step, the fractions are collected by adding a mixture of solvents of increasing polarity (Table 2). For each fraction a different glass flask is used.

Table 2.: Fractions and the solvents which are used in each sample.

Fraction	Elution solvent mixture	Homologous series
F1	*n*-hexane	Aliphatic hydrocarbons
F2	dichloromethane/ *n*-hexane (2:3)	Long chain alkenones
F3	ethyl acetate/*n*-hexane (1:2)	*n*-alkanols, sterols, diols, keto-ols

It should be pointed out that prior to GC-MS analysis *n*-alkanols and steroidal alcohols were derivatized to the corresponding trimethylsilyl ethers. The aforementioned procedure is called silylation and refers to the replacement of a reactive hydrogen atom in OH, COOH, SH, NH, CONH, POH, SOH or enolizable carbonyl with a silyl group and commonly with trimethylsilyl (TMS) (Fig. 6); (Moldoveanu & David, 2019). The silylation reaction is frequently utilised in Gas-Chromatography mainly in order to diminish the polarity of each analyte and increase its stability and to render the analyte more detectable (Moldoveanu & David, 2019). The chemical reaction of an analyte Y:H with the formation of a TMS derivative is presented below:

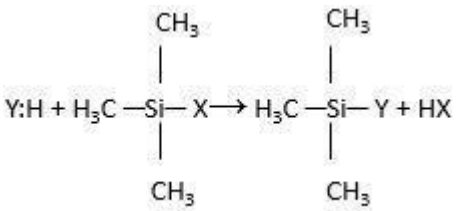

Figure 6.: The chemical reaction of an analyte Y:H with the formation of a TMS derivative (Moldoveanu & David, 2019).

The contents of the white vials with the fraction of the *n*-alkanols and steroidal alcohols, namely F3, were initially evaporated under a stream of nitrogen to dryness. After the total concentration 100 μL of N,O-bis-(trimethylsilyl)-trifluoroacetamide (BSTFA) was added into all F3 vials, then shook with a vortex device and let into the oven at 90°C for 1 hour. Following, the above mixture was placed afresh under a gentle nitrogen stream till dryness and ultimately 50 μL of isooctane was added into each sample for chromatographic analysis.

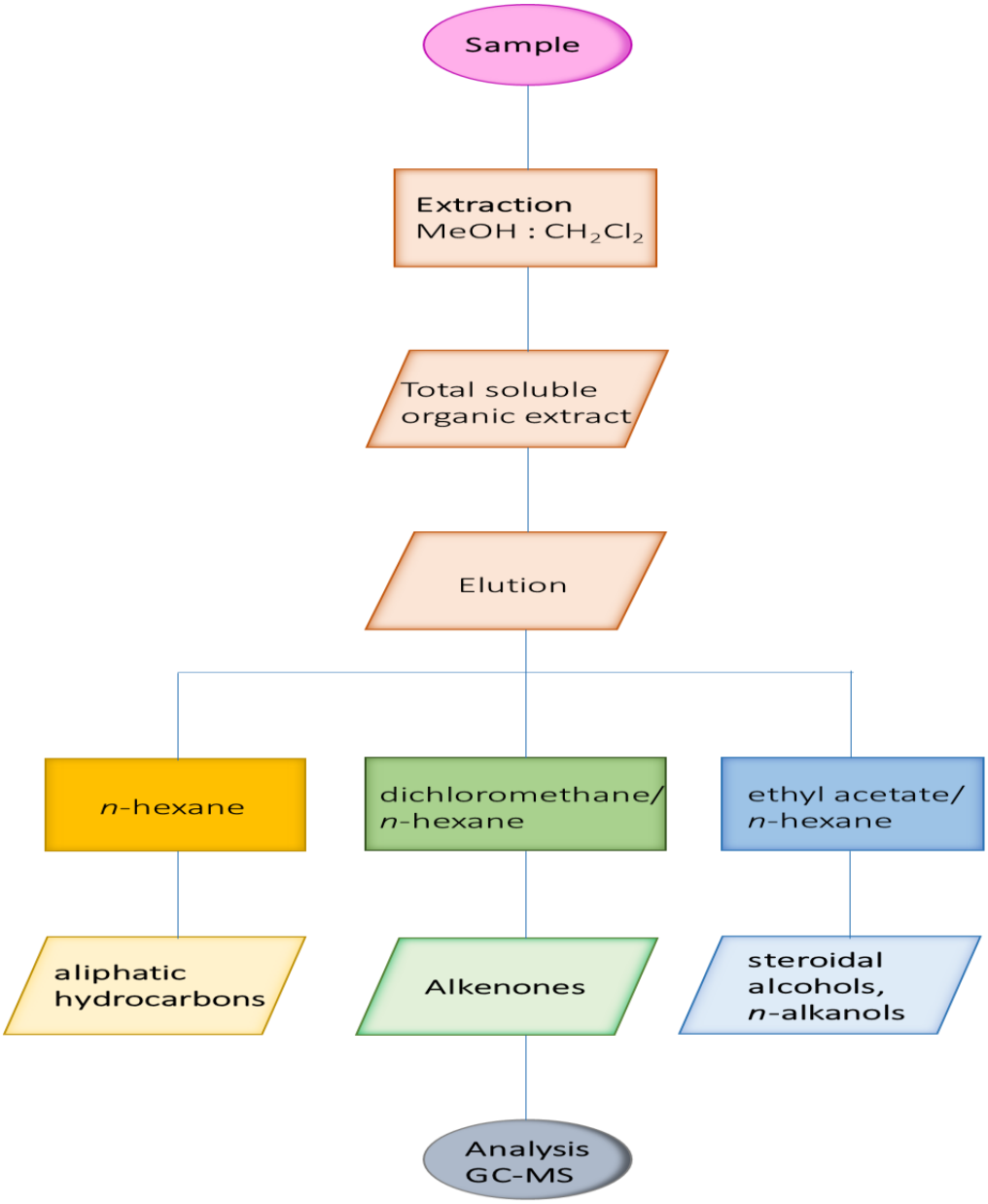

Figure 7.: Simplified schematic representation of the analytical procedure.

3.5. Identification and quantitative determination [GC-MS]

The analysis of the aforementioned organic fractions indicates that they are usually found in relatively low concentrations in environmental samples and for this reason the use of high precision analytical techniques is required.

The instrumental analysis for the determination of the organic substances in the study samples was carried out by gas chromatography - mass spectrometry (GC-MS) on an Agilent 7890 GC, which is equipped with an HP-5MS capillary column, with the characteristics 30m×0.25mm i.d. × 0.25 μm phase film, in combination with an Agilent 5975C MSD. Details regarding the instrumental analysis parameters can be found elsewhere (Gogou et al., 2007).

The aliphatic hydrocarbon fraction consists of the *n*-alkanes and the UCM. Pertaining to the *n*-alkanes, the homologues from *n*-C_{24} to *n*-C_{35} were identified/quantified. In the same vein, the long-chain alkenones with 37 and 38 carbon atoms and the *n*-alkanols from *n*-C_{14} to *n*-C_{30} were determined as well. Furthermore, alkanediols-1,15 (diols), keto-15-alkanols-1 (keto-ols) C_{30} and isololiolide and loliolide were identified. Ultimately, the cholesterol, brassicasterol, sitosterol and dinosterol steroid alcohols were also determined.

The individual lipid components were identified by a combination of comparison of GC-retention times to authentic standards and a comparison of their mass-spectral data to those in the literature. Quantification was based on the GC-MS response and achieved by comparison of peak areas with those of internal standards. The aforementioned process has been executed using the application 'Agilent MSD Productivity ChemStation for GC and GC-MS Systems, Data Analysis Application'.

The signal of the unresolved complex mixture (UCM) of aliphatic hydrocarbons was defined by the chromatographic area (fraction F1) between the solvent baseline and the curve defining the base of resolved peaks. UCM quantification was performed relatively to [$^2H_{50}$] *n*-tetracosane using the average response factor of *n*-alkanes over the range of *n*-C_{10} to *n*-C_{35} (Gogou et al., 2000; Parinos et al., 2013).

3.6. Lipid biomarkers and their application

The detailed examination of numerous lipid biomarkers in paleoceanographic studies enables the identification of both autochthonous and allochthonous sources contributing to sediment organic matter and provides information on the responses of marine and terrestrial ecosystems to anthropogenic pressures and land-ocean interactions (Gogou et al., 2007, 2016; Ouyang et al., 2015; Strong et al., 2013). The analysis of particular indices employed in this study is presented in detail below.

3.6.1. Hydrocarbons and alcohols (*n*-alkanes and *n*-alkanols) and indices

The sum of the concentrations of the most abundant high molecular weight *n*-alkanes and *n*-alkanols of terrestrial origin are defined as follows:

$$\text{TerNA} = n\text{-C}_{27} + n\text{-C}_{29} + n\text{-C}_{31} + n\text{-C}_{33} \quad (1)$$

and

$$\text{TerNOH} = n\text{-C}_{24}\text{OH} + n\text{-C}_{26}\text{OH} + n\text{-C}_{28}\text{OH} + n\text{-C}_{30}\text{OH} \quad (2)$$

The carbon preference index of long-chain *n*-alkanes (CPI_{NA}) has been used as an indicator of terrestrial organic matter degradation. In other words, CPI is the ratio of the concentrations of long straight-chain homologues with an odd number of carbon atoms to those with an even number. In the same vein, plant-wax derived n-alkanes have a typical carbon chain-length between *n*-C_{25} and *n*-C_{35} and show a strong predominance of odd-carbon homologues over even-carbon homologues with the most dominant representatives being the *n*-C_{27}, *n*-C_{29}, *n*-C_{31} and *n*-C_{33} (Eglinton & Hamilton, 1967). The magnitude of this odd-over-even predominance is expressed by the above index (Bray & Evans, 1961), which is used to distinguish between plant (CPI≥4 in plants) (Ohkouchi et al., 1997) and fossil fuel products (CPI~1) (Wang et al., 1999). Additionally, the alkanes of which the carbon chain consists of less than 20 carbon atoms and with greater abundance in homologues 15, 17 and 19 are derived from marine phytoplankton organisms or microorganisms (Sargent & Gatten, 1974). In each case, the indices were calculated as follows:

$$\text{CPI}_{\text{NA}} = \frac{n-\text{C}_{25} + n-\text{C}_{27} + n-\text{C}_{29} + n-\text{C}_{31} + n-\text{C}_{33}}{n-\text{C}_{24} + n-\text{C}_{26} + n-\text{C}_{28} + n-\text{C}_{30} + n-\text{C}_{32}} \quad (3)$$

Further, chain length variations, the average chain length-ACL, in land plant biomarker are commonly related to oscillations in the temperature and humidity/aridity in the growing environment of source vegetation, since plants tend to synthesise longer chain length waxy components in response to elevated temperatures (Poynter & Eglinton, 1990). Hence, changes in the vegetation cover during varied climatic periods could be inferred by changes in the average chain length of terrestrial *n*-alkanes (Kouli et al., 2012):

$$\text{ACL} = \frac{27 \times n-\text{C}_{27} + 29 \times n-\text{C}_{29} + 31 \times n-\text{C}_{31} + 33 \times n-\text{C}_{33}}{n-\text{C}_{27} + n-\text{C}_{29} + n-\text{C}_{31} + n-\text{C}_{33}} \quad (4)$$

In addition, the relation of the abundances of long chain *n*-alkanes and *n*-alkanols, namely HPA index; (Poynter & Eglinton, 1990), is utilised to determine the proportions of labile and refractory organic matter transported in the marine environment, and the *in-situ* preservation *vs.* degradation trends under various redox conditions as well (Gogou et al., 2016). The HPA index was calculated as follows:

$$\mathrm{HPA} = \frac{\mathrm{C24,26,28}\ n\mathrm{-alkanol}}{\mathrm{C24,26,28}\ n\mathrm{-alkanol} + \mathrm{C27,29,31}\ n\mathrm{-alkane}} \quad (5)$$

More specifically, the labile material has a great significance to biological productivity in the ocean, and is used up most rapidly (Altenbach, 1992). and moving onto the second mentioned form of organic matter, refractory organic carbon is almost biologically inert, has limited nutritious value and will commonly bypass the oxic niches at the sediment-water interface. In general, it should be pointed out that the sediment organic material is a residue from various physical processes and not always directly linked to biological productivity.

Another important ratio used in the present study is the relative proportion of *n*-hexacosan-1-ol (*n*-C_{26}OH) to the sum of *n*-C_{26}OH plus the most abundant *n*-alkane in the samples, the *n*-C_{31} homologue, *n*-C_{26}OH/ *n*-C_{26}OH+*n*-C_{31}. The aforesaid ratio constitutes a chemical proxy reflecting oxygenation associated with bottom current intensity, given that both compounds have the same origin (i.e., vascular terrestrial plants) but differed in resistance to degradation by oxygenation of the deep sea floor (Martrat et al., 2007).

The unresolved complex mixture (UCM) of aliphatic hydrocarbons abundance is utilised as an indicator of the contribution of anthropogenic organic matter from degraded petroleum hydrocarbons and/or apolar products deriving from combustion processes, for instance grass, wood and coal combustion and/or the incomplete combustion of fossil fuels (Hays et al., 2004; Simoneit, 1984; Wang et al., 1999). The aforesaid mixture refers to a commonly observed persistent contaminant mixture in marine sediments and environmental samples consisting of branched alicyclic hydrocarbons (Gough & Rowland, 1990), which has been proven toxic to sediment-dwelling organisms (Parinos et al., 2013; Scarlett et al., 2007). Finally, it's not possible for it to undergo separation by the chromatograph.

In addition, the relative abundance of UCM compared to the total resolved aliphatic hydrocarbons (UCM/TRes) is used as an indicator of the co-current presence of an enhanced petrogenic signal from non-extensively degraded petroleum products (Simoneit, 1984). Aliphatic compounds of crude oil and petroleum products released in aquatic environments are subjected to degradation, with a prominent initial microbial preference for straight chain compounds (Wang et al., 1999). This leads to the gradual removal of major compounds that can be resolved by gas chromatography and the subsequent appearance of a UCM. UCM/TRes ratio values >7 indicate chronic pollution from petroleum products, values <4 indicate an enhanced petrogenic signal from non-extensively degraded petroleum products in some cases (Simoneit, 1984). Finally, the UCM/TRes index provides info about the level of weathering or alteration that a hydrocarbon sample has undergone. Higher values indicate a

higher proportion of unresolved complex mixtures compared to resolved aliphatic hydrocarbons.

3.6.2. Long-chain alkenones

The U_{37}^{k} index, which has mentioned in the first chapter, is calculated from the relative abundances of C_{37} methyl alkenones containing 2-4 double bonds (Müller et al., 1998). Moreover, there is also the $U_{37}^{k'}$ index, which constitutes a very useful lipid-derived SST index based on long-chain di- and tri-unsaturated alkenones with 37 carbon atoms ($C_{37:2}$ and $C_{37:3}$, respectively) and excludes the tetra-unsaturated alkenone ($C_{37:4}$) from the calculation. In this respect, the $U_{37}^{k'}$ index is defined as the ratio of di-unsaturated alkenone to the sum of di- and tri-unsaturated alkenones [($C_{37:2}$/ ($C_{37:2}$+$C_{37:3}$)].

$$U_{37}^{k'} = \frac{C_{37:2}}{C_{37:2} + C_{37:3}} \quad (6)$$

Through extensive studies the $U_{37}^{k'}$ index appeared to provide preferable regressions related to *in situ* Sea Surface Temperatures than U_{37}^{k} and constitute the most broadly utilised SST proxy (Zheng et al., 2016). The $C_{37:4}$ alkenone was initially included in calculations, since it was thought that it may convey some temperature information as well (Marlowe et al., 1984). (Prahl & Wakeham, 1987) excluded the $C_{37:4}$ alkenone from the equation because it is often not detectable in sediments (Brassell et al., 1986) and its exclusion improved the linearity of the relationship at lower temperatures (Prahl et al., 1988; Sikes et al., 1997). Nevertheless, recent studies have exhibited that including $C_{37:4}$ alkenones for lacustrine or brackish water haptophytes, such as *Ruttnera* (*Chrysotila*) *lamellosa* and *Isochrysis galbana* improves temperature correlations although notable deviations at the extreme high and low temperatures can still be observed. In cultures, field measurements and sediments, it is observed that the relative proportion of $C_{37:3}$ increases with decreasing ambient temperature (Van der Meer et al., 2013).

Pertaining to calibration, a single calibration may not be applicable in all oceanic regions. For paleoceanographic purposes, it is vital that a sediment-based $U_{37}^{k'}$ temperature calibrations should be established in order to define the most reliable relationship for a given vicinity (Müller et al., 1998). Sediment-based calibrations have an advantage over culture and particulate matter studies because they implicitly consider changing oceanic settings, species distributions, and diagenetic environments. Moreover, seasonality can limit our ability to interpret paleotemperatures and paleoenvironmental information from the $U_{37}^{k'}$ signal in sediments and researchers should take it into account (Sikes et al., 1997). Further, local field calibrations are better to be utilised, however, the similarity of field calibrations suggests that the range in open ocean variations is sufficiently narrow that the use of a single worldwide calibration is within acceptable limits (Müller et al., 1998). Nonetheless, field calibrations of the technique have demonstrated that the relationship between $U_{37}^{k'}$ and temperature is

remarkably consistent and linear with SST in the world's oceans over a broad temperature range, namely 5-25°C (Sikes et al., 1997).

The aforementioned technique constitutes a valuable asset in the paleoceanographic studies, since it is the first quantitative method for SST estimation that is not based on microfossil shells. For this reason, it augments established techniques because it refers to a different set of environmental controls than those that influence foraminiferal assemblages or isotope values (Sikes et al., 1997). The proportions of long-chain unsaturated ketones on which $U_{37}^{k'}$ is based vary depending on the organisms responding to the water temperature in which it is growing (Prahl et al., 1988) and thus is distinct from other geochemical temperature proxies such as $\delta^{18}O$ which are based on passive, equilibrium processes.

Finally, the $U_{37}^{k'}$ paleothermometer has been successfully applied for SST reconstructions since the Late Pleistocene, in high-resolution studies covering the Holocene and in combination with other SST indices (Herbert, 2003).

Among the different calibrations available (see Tierney & Tingley, (2018) for a recent review), for the present study, the alkenone unsaturation index measurements in core-top sediments of the Mediterranean region show a good match with present average annual SST data when calculated using the global calibration of (Conte et al., 2006) :

$$T = -0.957 + 54.293 \times \left(U_{37}^{k'}\right) - 52.894 \times \left(U_{37}^{k'}\right)^2 + 28.321 \times \left(U_{37}^{k'}\right)^3 \qquad (7)$$

The uncertainty reported for the calibration of alkenone and SST is ca. 1.1°C at a confidence level of 68% (Conte et al., 2006), which represents part of the uncertainty associated with the reconstruction, to be added to the analytical error that it is <0.5ºC.

It is well known that in the Aegean Sea, coccosphere fluxes reveal that the main alkenone producer, namely *Emiliania huxleyi*, constitutes the dominant species throughout the year with the higher production and export rates occurring between March and June and a secondary maximum from June to November (Malinverno et al., 2009). Consequently, the estimated alkenone patterns and accordingly the reconstructed alkenone SSTs are assumed to reflect mean annual temperature values. Apart from the $C_{37:}$ alkenones, $C_{38:}$ alkenones are also detected in the sediments, though their chromatographic separation is more challenging than for the $C_{37:}$ homologues. As an example, the long-chain alkenones identified in S25_1 multicore are given in Table 3 and a characteristic chromatogram of the determined alkenones is depicted in Fig. 8.

3.6.3. Steroid alcohols

Marine sterols are major constituents of several marine phytoplankton groups (Menzel et al., 2003; Volkman et al., 1999). The sterols used as marine biomarkers in the current study consist of cholesterol, brassicasterol, sitosterol and dinosterol. The systematic names and abbreviations (with structural information: number/position of double bonds) of the sterols detected in the sediments of the S25_1 core are shown in Table 3.

Table 3.: Nomenclature of the steroidal alcohols in the S25_1 core.

Abbreviation	**IUPAC nomenclature**	**Other name**
27Δ^{5}	cholest-5-en-3β-ol	cholesterol
28Δ^{5,22E}	24-methylcholesta-5,22-dien-3β-ol	brassicasterol
29Δ^{5}	24-ethylcholesta-5-en-3β-ol	sitosterol
30Δ^{22E}	4*α*,23,24-trimethyl-5*α*(H)cholest-22(E)-en-3β-ol	dinosterol

The sum of concentrations of the considered lipid biomarkers of algal origin was calculated as follows:

$$\Sigma Algal = 28\Delta^{5,22E} + 30\Delta^{22E} + C_{30,}diols\&keto\text{-}ols + C_{37,}alkenones + loliolide + isololiolide \quad (8)$$

4. Result

4.1 SSTs

Alkenone-derived SSTs provide a record from 611 to 2014 y CE, according to the age model, at the Epidaurus Basin (Fig. 8, 9). Values vary from approximately 18.8°C (traced back to around the beginning of the 8th century, ca. 710 y CE; high confidence, ^{14}C pointer ca. 610.5 y CE; cm 46) to 25.3°C (recorded by the end of the 18th century; very high confidence, ^{14}C pointer ca. 1730 y CE; cm 11). This gives a range of 6.4°C difference.

In more detail, in the early 7th century the temperature was at 20.2°C, while in approximately 630 y CE a temperature increase of about 2°C was observed. Further, roughly for the following 85 years, an average temperature of 21.7°C prevails until in the beginning of the 8th century a sharp decrease of >3°C is presented and the aforementioned minimum peak of 18.8°C is being noted. In 780±30 y CE there was an increase of about 3.5°C, i.e. from 19°C in the mid of 8th century it increased to 22.5°C. Then there was a new decrease to 20.2°C, and then the temperature gradually increased and reached 23.2°C in 950±30 y CE and by the first decades of the 11th century there was another decrease of about 2.5°C, more specifically 20.6°C.

Immediately after 1050±30 y CE it reached 22.2°C again and until the last decades of the 13th century several fluctuations were observed with an average temperature of 22°C and a range of temperatures from 21.3 to 22.8°C. From ca. 1280 y CE on, a distinct increase in temperature is recorded reaching 24.6°C in the first decades of the 14th century and until approximately 1420 y CE it decreases considerably and specifically by about 4°C and reaches 20.4°C. Then until the beginning of the 17th century 1600±30 y CE there were relatively stable temperatures with an average of 21°C and particularly in the period from 1420 to 1600±30 y CE the positive maximum was in 1517±30 with 21.9°C whereas in the mid of 16th century a negative maximum was encountered at 20.1°C. From 1600±30 y CE to the middle of the 18th century an incremental tendency from the previously highest temperatures is shown and during this period there are fluctuations with an average of 23.1°C. Reduced values down to 22.3°C are observed in 1755±30 y CE and then they rise again in ca. 1795 y CE to 25.3°C.

Since 1800 y CE interval fluctuations of a smaller range are observed. From the early 19th century to the mid-19th century relatively constant temperatures at 22.8°C were recorded. In 1885±30 y CE one of the largest increases to 24.9°C was presented and is among the highest temperatures in the dataset. A notable decrease to 22.7°C appears in about 1900 y CE, which remains relatively constant at 22.8°C until 1925±30 when it decreases again down to 21.5°C in 1940±30 y CE. An increase to 23.6°C in 1950±30 y CE is noted followed by a decrease with small fluctuations until 2014 with an average of 21.7°C.

4.2. Marine input (alkenones and algal concentration)

Pertaining to the alkenones, their concentrations range from 22.3 to 658 ng/g (Fig. 9). The minimum value of 22.3 ng/g is noted at the end of 10th century, while the maximum of 658

ng/g is shown in the middle of the 20th century. From the beginning of the dataset the values are presented as relatively stable until the middle of the 18th century and with small-scaled fluctuations. From the end of the 18th century until approximately 1830±30 y CE, the total alkenone concentration values were quite low with a mean value approximately 60 ng/g. After the aforesaid period a sharp increase in values is observed until 1885±30 y CE with 320 ng/g, followed by a sharp decrease to 17.1 ng/g in ca. 1900 y CE. Further, a positive trend until the mid of 20th century with 658 ng/g is observed, decreasing anew by 491 ng/g in 1975±30 y CE with 167 ng/g and till the top of the core the mean value was about 243 ng/g, i.e. higher than the mean value of the whole dataset which was about 100 ng/g.

The highest value of dinosterol concentration is noted in the last sample of the dataset (2014±30 y CE) with 434.8 ng/g and the lowest in 812±30 y CE with 15.3 ng/g. From the beginning of the 7th century until ca. 1680 y CE the values of dinosterol concentration show a relatively stable path with an average value of 40.8 ng/g. From approximately the second half of the 17th century until about the middle of the 19th century, dinosterol concentration shows the mean value 141 ng/g and a gentle increase is presented until 1820±30 y CE with the biggest peak in the last decades of the 18th century with 316ng/g. The decades after 1820 y CE mark an immense increase of dinosterol concentration from 142 ng/g in 1820±30 y CE to 356 ng/g in 1885±30 y CE. Further, from 1885±30 y CE until the first decade of 20th century a decreasing trend of approximately 135 ng/g is observed and during the 20th century the values exhibit an increasing trend anew. Besides, the new millennium values have an incremental tendency as well with the highest values of all dinosterol dataset (Fig 9).

The maximum value of sitosterol is 469 ng/g in the beginning of the 21thcentury, the minimum is 25.1 ng/g in 780±30 y CE and the mean value of the whole dataset is 137 ng/g (Fig. 9). From the lowest part of the core until 1150±30 y CE several fluctuations are noticed. After the previously mentioned time period and till ca. 1280 y CE a sharp increase is observed which is followed by a decreasing trend until 1350 y CE. During the mid-14th century until the end of the 16th century a relatively stable situation took place. After 1600±30 y CE an incremental tendency with several fluctuations and in general higher values related to the rest of the dataset values is observed until the top of the core, especially after 1846±30 y CE, whence the average value until 2014±30 y CE is 276 ng/g.

The minimum cholesterol value in the current dataset is 11.0 ng/g in 630±30 y CE and the maximum value is 552 ng/g in the most contemporary sample in 2014±30 y CE (Fig. 9). From 611±30 y CE till the second decade of the 19th century the values are presented relatively stable with several fluctuations and the maximum value of this interval in 1250±30 y CE with approximately 83.0 ng/g. After 1820±30 y CE an incremental tendency is noticed with a gentle oscillation pattern until the last decades, where both the highest increase and the highest value are shown. The mean value of the whole dataset is roughly 68 ng/g, the average value in approximately the last 140 years, namely 1870±30 y CE and upwards, is about 190 ng/g and the mean value of the first 1260 years is approximately 36.0 ng/g.

The minimum brassicasterol value in the current dataset is 6.26 ng/g in approximately 630 y CE and the maximum value is 174 ng/g in 2014±30 y CE (Fig. 9). From the bottom of the core until 1350 y CE several fluctuations are observed, and the mean value is 17.1 ng/g. From

1350±30 till 1600±30 y CE a stable pattern is presented with a mean value of 15.8 ng/g and from 1600 until ca. 1830 y CE the values are relatively stable as well with slight oscillations. From 1830±30 y CE until the top of the core an incremental trend is shown with an average value of approximately 109 ng/g and the highest values in the dataset. Finally, a decreasing pattern is observed between the interval between 1885 and 1910±30 y CE with values 135 ng/g to 22.3 ng/g respectively.

The sum of algal biomarkers (ΣAlgal) varies between 0.23 and 4.35 μg/g and has a mean value of 0.90 μg/g (Fig. 9). As is shown, from the bottom of the core until the first three decades of the 19th century the vertical profile of ΣAlgal has almost constantly low values with a mean value of 0.57 μg/g, with two positive peaks in the middle of the 10th century with approximately 1 and in the middle of the 13th century with roughly 1.34 μg/g. After the aforementioned period and for the next decades, the values of ΣAlgal rise promptly to mean value of 1.89 μg/g. During the 20th century there were some fluctuations in the concentration of ΣAlgal, notwithstanding an incremental trend is observed. The minimum value for this period was about 1.03 μg/g in the early 20th century, while the maximum was about 4.35 μg/g in 2000 y CE.

4.3 Terrestrial input (*n*-alkanes and *n*-alcohols indices)

TerNA values range from 0.49 to 1.64 μg/g, the mean value is 0.97 μg/g, while TerNOH ranges from 0.28 to 1.40 μg/g, averaging 0.59 μg/g (Fig.8). In general, TerNA and TerNOH show similar fluctuations and patterns with some exceptions, e.g. in 1420±30 y CE, where TerNA increases, while TerNOH decreases. For both graphs the minimum values are observed at the bottom of the core, particularly in 695±30 y CE, while the maximum value of TerNA at the middle of the core is observed in 1420±30 y CE and of TerNOH at the top of the core around 2000 y CE. As previously mentioned, the two indices show almost identical patterns, with the exception of points such as 1330±30 y CE, where the TerNOH showed a decreasing trend from 1285±30 y CE, while the TerNA showed an increasing trend and the corresponding phenomenon occurs in approximately 1570 y CE as well. Further, it is worth mentioning that from 695 to 780±30 y CE an increase of terrestrial inputs is noted and it was followed by a decrease until the first decade of the 9th century. Afterwards, an increasing trend with marked periods of oscillations for TerNA and TerNOH concentrations is evident from the first decades of the 18th century until ca. 1900 y CE and an incremental tendency is observed with several fluctuations from 1900 y CE until present.

The ACL index of *n*-C_{27} – *n*-C_{33} *n*-alkanes varies between 29.78 in 1180±30 y CE and 30.51 in 1755±30 y CE (Fig. 8). During the pre-Industrial period, namely before 1750 y CE, ACL values remained relatively constant and some intervals were near an oscillation pattern, e.g. from ca. 1250 till approximately 1380 y CE. Eventually, from the onset of the 20th century until the middle of it, a tiny rise in the values is presented, while in the last decades the fluctuations appear to be milder.

Related to the HPA index, the maximum value is 0.77 in 1420±30 y CE, the minimum is 0.42 in modern 2000 y CE, according to the age model, and the mean value of the whole dataset is

0.62 (Fig 8, 9). The values are generally stable with a lot of fluctuations and oscillation patterns. Distribution of HPA gently follows that of ACL index in general.

Pertaining to the C_{26}OH% index, fluctuations are observed throughout the dataset from 611 to 2014 y CE (Fig. 8, 9). The average value is 0.34 and the range of values is from 0.19 in 1420±30 y CE to the highest value of 0.56 noted in 2001±30 y CE. Since 1950 y CE, increased values are shown in comparison with the rest of the data set and fluctuations are presented as well. Finally, the biggest increase is observed in 1420±30 y CE whence the value increased by 0.3 up until one century later, namely in around 1520 y CE.

The CPI_{NA} values of high molecular weight *n*-alkanes range from 4.03 in 2014 to 16.77 in 1015±30 y CE (Fig. 8). From the beginning of the dataset, namely the early 7th century till the end of the 16th century there is an average value of 12.14 with the maximum interval peaks in ca. 1015 y CE with a value of 16.8 and in 1485±30 y CE with 16.2 and minimum interval peaks in 1050±30 y CE with 9.9 and in 1320 y CE with 9.8. From around 1600 y CE a gradual decrease in CPI_{NA} values was observed until ca. 1680 y CE. The last decades of the data set are characterised by several fluctuations and generally lower values related to the rest of the dataset with the lowest values in 2014±30 y CE. More specifically, the mean CPI_{NA} values show a sudden drop of 5.32, namely in 6.82.

UCM values vary between 0.02 μg/g in 1517 and 42.9 μg/g in ca. 1950 y CE (Fig. 8). From the early of the 7th century until approximately 1850 y CE low concentrations are shown and then the UCM values increase onwards to 2014±30y CE.

The UCM/TRes chart follows a similar pattern to the UCM chart with minor variations (Fig. 8). More specifically, the average value is 3.5 and the range of values observed is from 0.02 in 1520±30 y CE with a max value of about 8.6 in the mid-20th century.

It should be pointed out that the values of the above organic compounds rose after the last decades of the 19th century until present, compared to the very low concentrations demonstrated before this period.

Below, the table 5 is showing the main age intervals of the dataset and the trend, the mean value and the standard deviation of SST, TerNA, CPI_{NA}, Algal concentration and C_{26}OH% index. The charts were created under the guidance of Dr. Belen Martrat.

Table 5.: Statistical parameters of SST, TerNA, CPI_{NA}, UCM, Algal concentration and $C_{26}OH$ values of the main age intervals of the last 1.5k.

		Dark Ages (611-950)	**MCA (950-1250)**	**LIA warming phase (1250-1500)**	**LIA cooling phase (1500-1850)**	**Last bin (1850-2014)**
	trend	↑	↑	variability	↑	↓
SST	mean (◦C)	21.2	22.1	22	22.8	22.6
	St.Deviation	1.43	0.73	1.38	1.29	1.05
	trend	variability	↑	↑	variability	↑
TerNA	mean(μg/g)	0.89	0.97	0.97	0.88	1.13
	St.Deviation	0.28	0.18	0.36	0.20	0.23
	trend	steady	steady	steady	↑	↑
UCM	mean(μg/g)	0.48	1.27	0.93	12.3	28.7
	St.Deviation	0.38	2.06	0.89	8.42	7.75
	trend	↑	variability	↓	↓	↓
CPI_{NA}	mean	12.47	12.25	11.82	7.99	6
	St.Deviation	1.41	1.93	2.06	2.55	1.38
	trend	steady	↑	↓	↑	↑
Algal	mean(μg/g)	0.44	0.61	0.54	0.72	1.89
	St.Deviation	0.20	0.32	0.30	0.28	0.84
	trend	steady	↑	↓	↑	↑
$C_{26}OH$	mean %	31.2	32	29.9	36.4	38.5
	St.Deviation	0.04	0.04	0.07	0.05	0.08

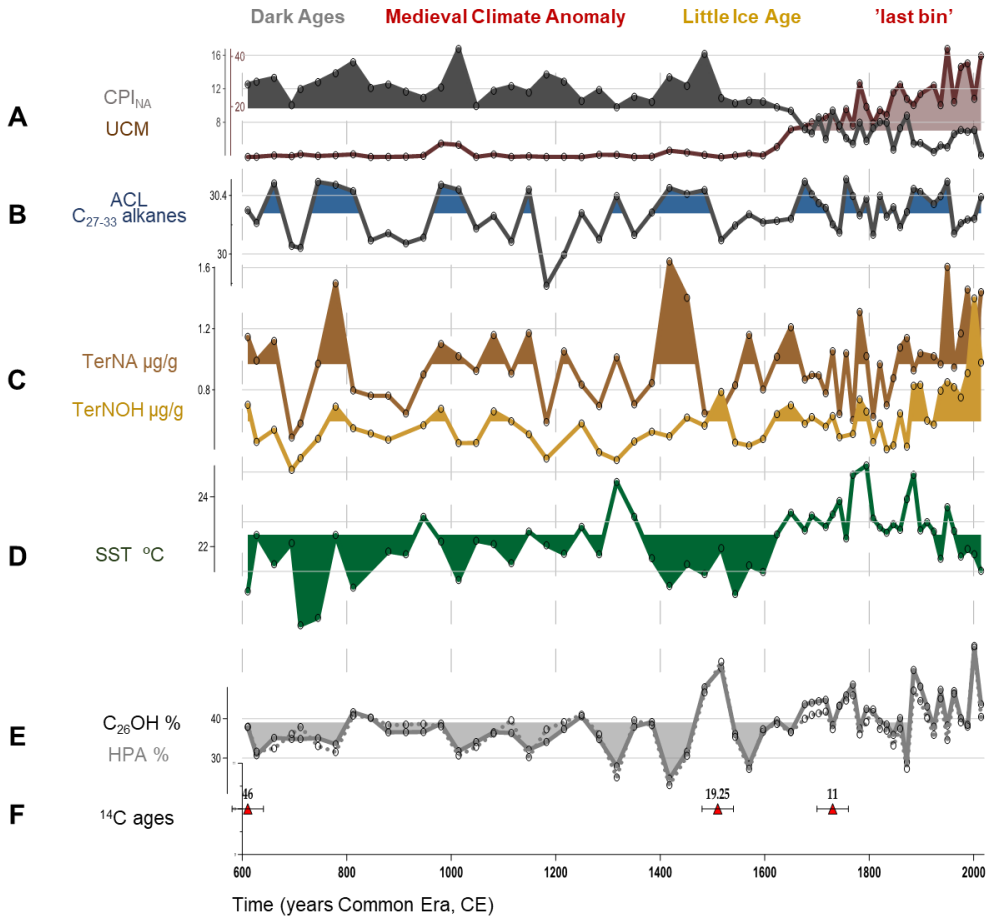

Figure 8.: Paleo-dataset in Epidaurus Basin sediments over the last 1500 years. (A) CPI_{NA} and UCM and (B) ACL (C_{27-33} alkanes) and (C) TerNA and TerNOH (µg/g) and (D) Sea Surface Temperature (SST) (◦C) using alkenones and (E) Relative proportion of *n*-hexacosan-1-ol (*n*-C_{26}OH) to the sum of *n*-C_{26}OH plus *n*-C_{31} and HPA index and (F) ^{14}C age pointers with 1σ error.

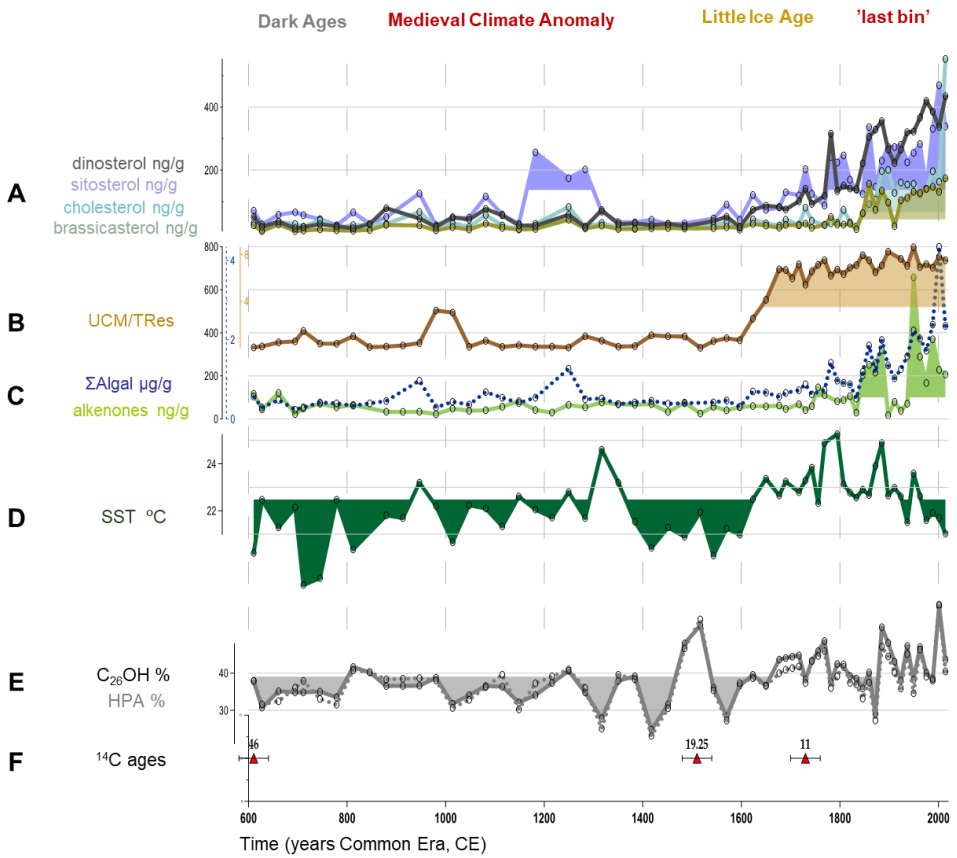

Figure 9.: Paleo-dataset in Epidaurus Basin sediments over the last 1500 years. (A) steroidal alcohols (dinosterol, sitosterol, cholesterol, brassicasterol (ng/g) and (B) UCM/Tres and (C) algal (µg/g) and alkenones (ng/g) concentration and (D) Sea Surface Temperature (SST) (◦C) using alkenones and (E) relative proportion of *n*-hexacosan-1-ol (*n*-C_{26}OH) to the sum of *n*-C_{26}OH plus *n*-C_{31} and HPA index and (F) ^{14}C age pointers with 1σ error.

5. Discussion

Seasonal and spatial climate information for each vicinity contains several unique parameters and is not perfectly applicable as climate models to all regions. Therefore, in the process of reconstructing climate, after various methods and data have been processed, one factor that must be seriously taken into account is uncertainty.

Further, it should be pointed out that in the Mediterranean area many studies have been conducted pertaining to paleoclimate reconstruction from both marine and continental material and the data presented vary considerably depending on the area, as the Mediterranean is a quite active region with many parameters that are able to drastically change the circulation and climate between the regions (Gogou et al., 2016; Roberts et al., 2012). Below are presented in detail the conditions that prevailed in the period 611-2014 y CE, according to the age model, in the area of Epidaurus through the analysis of the multicore S25_1, as well as comparisons with other areas of the Mediterranean.

DA (600-950 y CE)

Climatic and environmental proxy reconstructions of the S25_1 record reveal a cooling trend from about 695 to 740 y CE with a decrease of 3°C followed by a warming trend late-8th century. Regarding the TerNA and TerNOH values, namely the terrestrial inputs concentrations, high values are presented, followed by high CPI_{NA} ratio values. The CPI_{NA} ratio shows high values throughout the age interval of the current dataset, and it drops after approximately the early of the 20th century due to the introduction of the anthropogenic impact (fossil fuels/petroleum combustion). The high CPI_{NA} values (average around 13) of this age interval denote a preserved terrestrial signal.

More specifically, as regards the sum of terrestrial *n*-alkanes, namely the TerNA values, the highest value of the interval is observed in 779±30 y CE (with 1.5 μg/g) and the lowest in 695±30 y CE (0.5 μg/g). Therefore, in the interval ca. 695-780 y CE the terrigenous inputs are slightly increased (0.88 μg/g), which is probably due to riverine runoffs and a change of climate to wetter conditions. This is also confirmed by sitosterol values which itself comes from both marine and terrestrial origin and shows a slight increase in contrast to the other sterols which are only found in marine environments and by the minor increase of the ∑Algal concentration.

In the same period an increase in SST from 18°C to 22.5°C is noted, namely increased ACL values. Hence, since an increase in temperature is shown and a rising trend in HPA values as well, it is indicated that there is a high preservation of organic matter due to reduced water mixing in the area. This is consistent with previous studies that suggested eastern-western hydroclimate see-saws (Roberts et al., 2012).

During the 9th to 10th centuries, there were fluctuations in SSTS' values, which hovered around an average of 22.2°C. These temperature changes coincided with an increase in marine algal inputs, likely due to a rise in nutrient availability from the influx of terrestrial material, which fact is observed by the TerNA and TerNOH values. Some events of SST decreases were linked to the presence of fresh organic matter, water stratification, and the

effective preservation of organic matter, as indicated by CPI_{NA} values, *n*-C_{26}OH and HPA percentages.

MCA (950-1250 y CE)

During the MCA in Epidaurus Basin in general, there is an upward trend in SST, constant values of terrestrial inputs with an average TerNA value of 0.71 μg/g, namely not so arid conditions are dominant, and a slightly increase in fresh organic matter, while as the beginning of the 13th century is approached, a decrease in SST and drier conditions (wetter than LIA) are observed. Furthermore, regarding the ca. 1000-1200 y CE interval of the MCA, values oscillate above this average, showing an increasing SST trend of 2^{o}C, consistent with other profiles of the western Mediterranean (Sicre et al., 2016). In more detail about the MCA in the Epidaurus Basin, there is a slight decrease in HPA values and up to 1000 y CE it is observed constantly, so the organic matter appears more degraded, which is reasonable as the fresh continental material decreases and may also enhance water mixing conditions in the region. By 1000±30 y CE the temperature decreases by 2.6^{o}C. There is also an increasing trend in temperature and as we approach 1200 y CE the supply of terrestrial material decreases slightly compared to the rest of the age interval (1150-1180±30 y CE).

During the MCA in the Adriatic Sea (core INV12-15) higher temperatures were recorded compared to the Epidaurus Basin, namely 22.6^{o}C compared to 22.1^{o}C, but generally warm conditions prevail (Jalali et al., 2018). Moreover, warm conditions during this interval are observed as well in the Balearic Sea from the core HER-MC-MR03_3 (Cisneros et al., 2016). The average temperature was 17.9^{o}C while the overall average for the dataset was 17.7^{o}C (990-1740±30 y CE). Another study from Alboran Sea (cores TTR-17-1_384B and TTR-17-1_436B) showed a drier climate during the MCA event with average temperatures of 19.3^{o}C and 19.1^{o}C respectively for the 2 cores (Nieto-Moreno et al., 2013).

Finally, regarding the UCM index, an increase is observed by the end of the 10th century. This increased value may have occurred due to some past fire events in the area, as a slight increase of the terrestrial inputs is also observed. Further analyses including polycyclic aromatic hydrocarbons (PAHs) and levoglucosan would be needed to confirm this.

LIA (ca. 13th-19th centuries y CE)

The LIA period is characterised by two distinct phases based on inputs from both marine and terrestrial sources. The first phase of LIA, which occurred roughly between the 13th and 16th centuries, was characterised by a warming trend. On the other hand, the second phase of the LIA, which took place around the 16th-19th centuries, witnessed a cooling trend.

During the LIA warming phase (ca. 1250-1500 y CE), there is a trend of warming SST. From approximately 1320 y CE onwards a rapid decrease in SST is noticed and as we reach the beginning of the 13th century, riverine runoff increases slightly and according to the *n*-C_{26}OH and HPA indices there is an enhanced preservation of terrestrial organic matter, so reduced water mixing. The *n*-C_{26}OH index, in line with the HPA index, provides information about alternate periods of organic material preservation (as a result of stratification of the water column) and non-preservation (higher ventilation) in the Epidaurus Basin. The latter condition, enhanced bottom water ventilation in the region, was associated with surface water freshening in the Sicily Channel, strengthened Mediterranean thermohaline circulation

and occurred with positive NAO and negative AMO phases, together with clusters of reduced solar activity and more frequent and strong volcanic eruptions (Incarbona et al., 2016). Furthermore, in ca. 1250 y CE an increase both in sitosterol and in the concentrations of Algal is presented which coincides with the weak water mixing revealed through the HPA index, so enhanced preservation of the terrestrial organic matter is recorded.

From the beginning of the 14th century until the second decade of the 15th century a SST cooling trend of almost 4.5^{o}C is presented which is followed by a relatively increasing trend until ca. 1600 y CE. The aforementioned warming period is in line from approximately 1520 y CE with HPA index so it refers to better preservation of terrestrial organic material likely due to water stratification. The concentrations of the terrestrial biomarkers increase sharply from 1385 to 1420±30 y CE and this suggests a transition from arid to more humid environmental conditions and it can be seen by the concomitant increase in sitosterol values, which has both marine and terrestrial origins (Volkman, 1986). The study of Jalali et al., (2018) from the Adriatic Sea has shown higher SST average value (22.5^{o}C) compared to the Epidaurus Basin (22^{o}C) and in general an increasing trend is observed during the LIAa event. Further, the research of Nieto-Moreno et al., (2013) has shown that at the end of the MCA event and towards the beginning of the LIA event there is an increase in terrestrial input (1300±30 y CE) at the Alboran Basin, as observed in the Epidaurus Basin.

Regarding the LIA cooling phase (ca. 1500-1850 y CE), in 1600±30 y CE there was a sharp and continuous increase in UCM and a decrease in CPI_{NA} values. This is probably due to the enlargement of the settlements of the area and probably increased wood burning, which explains the fact that the CPINA values do not decrease rapidly, as burning does not affect them as much as UCM from fossil fuel products. The HPA index shows a relatively negative trend and this leads to declining of terrestrial organic matter preservation related to the previous years and probably better sea-bottom oxygenation. During the same period and until the middle of the 18th century, depleted TerNA and TerNOH values, suggest more arid climatic conditions than within the MCA. In addition, since 1600 y CE, an increase in Algal concentration and marine productivity is also marked which indicates more nutrient availability.

From ca. 1800 y CE a continuous increase in algal concentration and marine sterols are presented, which demonstrates enhanced continental inputs resulting in higher productivity. The aforementioned increase is consistent with an abrupt increase in UCM, likely resulting from the enlargement of settlement in the area. Since 1800±30 y CE a slight transition to wetter condition is noted consistent with higher supply from continental/riverine runoffs rising precipitation and a degradation of organic matter, thus better water mixing. Finally, throughout the 18th century and for the first approximately 40 years the SSTs stabilised at a mean temperature of 23^{o}C.

Furthermore, from the mid-18th century there was an abrupt rise in SST from 22.3^{o}C to 25.3^{o}C in 1795±30 y CE which was followed by a distinct negative trend until around 1830 y CE. The aforesaid cooling trend may be probably synchronous to the LIA. In Epidaurus Basin, at the end of the LIA event, a relatively stable situation pertaining to the SST is noticed, in contrast to the Gulf of Lions (Sicre et al., 2016), where the SST showed a warming trend. In general, the LIA years, namely 1500-1850±30 y CE, show a positive trend in the first centuries so this event did not affect the Epidaurus Basin to a large extent.

The previously mentioned warming tendency from 1755 to 1795±30 y CE is probably a result of several hydrological alterations in the region of the Epidaurus Basin, suggested by the sudden rise of terrestrial and marine (alkenones and algal productivity) biomarker concentrations, as observed in the studies of (Martín-Puertas et al., 2010; Nieto-Moreno et al., 2013) and is in line with increases of the HPA index, indicating higher preservation of terrestrial organic matter due to reduced water column mixing. Additionally, in the Adriatic Sea, a decrease in temperature with an average of 22.5°C to 22.04°C is observed during the transition of LIAa to LIAb (Jalali et al., 2018). The same pattern is presented in the Balearic Sea (from 17.7°C to 17.4°C) (Cisneros et al., 2016), but also in the Alboran Sea from 17.6°C to 17.8°C. However, in the Epidaurus Basin and in the Alboran Sea (Pallacks et al., 2021) there is an upward trend from 22°C to 22.8°C and 17.6°C to 17.8°C respectively.

In addition, in 1815 y CE the eruption of the volcanic Tambora is not evident in the S25_1 multicore of Epidaurus Basin on the contrary to multicore M2 from Athos Basin (Gogou et al., 2016) and KSGC-31 from Gulf of Lions (Sicre et al., 2016).

Last bin (1850-2014 y CE)

The Industrial Era in Greece occurred a little late compared to the major European countries and, more specifically, it is observed around 1910-1930 y CE in the major cities of the country. In the wider area of the Epidaurus Basin, the beginning of the Industrial Era is observed around 1940 y CE, as the area is located away from major cities and harbours (Kontoyiannis et al., 2023). The largest increase in UCM values is observed starting in approximately 1940 y CE ranging from 20.6 μg/g to 43 μg/g in the mid-20th century and a major decrease in the CPI_{NA} index from 7 in 2001±30 y CE to 4 in 2014±30 y CE is noted as well. Moreover, the transition of the area towards an environment, with increasing human-induced pressures and in particular due to enhanced inputs of anthropogenic hydrocarbons deriving from the combustion of coal and fossil fuel products to the wider study site, occurs quite slowly.

Furthermore, increased values of TerNA and TerNOH indices are shown with mean values of 0.93 μg/g and 0.55 μg/g respectively from the early 7th century until 1940±30 y CE compared to 1.23 and 0.93 μg/g respectively in the years from 1940-2014±30 y CE, which presumably indicates an increased flow of continental material through atmospheric deposition or due to wetter conditions in the aforementioned period. Further, in the aforesaid age interval both higher concentrations of marine derived sterols (e.g. cholesterol, brassicasterol) and increased values of ΣAlgal have been recorded and may be due to increased nutrient availability. By the same token, the above parameter reinforces the conclusion that there are continental discharges in the study area and consequently increased productivity.

In addition, pertaining to SST, in the 19th century, a rise of approximately 2°C was observed, while in 1885±30 y CE cooling trend was presented. This may be the result of a combination of local climatic parameters and major physical geographical controls. The ACL ratio values shows a different pattern, so the alterations are exclusively related to marine processes. Furthermore, as we entered the 20th century, a pattern of declining SST and increasing HPA and *n*-C_{26}OH values ware observed in the region. This decline can be attributed to increased inputs of terrestrial materials and freshwater, as indicated by corresponding indices, as well due to a combination of local physicochemical processes and characteristics of the wider region of the Saronikos Gulf. Moreover, the SST values have shown a negative trend during the last decades of the current dataset, on the contrary to the M2 core of the Athos Basin

(Gogou et al., 2016), which shows a positive trend the last few years. Another study of the St407 core in Sicily shows a decrease in SST values during the last bin. In particular, the average SST value during this period was 16.9°C, while the average SST in the aforesaid age interval was 16.4°C (Incarbona et al., 2016). Moreover, the two cores from Alboran Sea, namely TTR-17-1_384B and TTR-17-1_436B (Nieto-Moreno et al., 2013), showed that humid conditions prevailed at the beginning of the last bin, yet since the middle of the 20th century there has been a decrease in terrestrial inputs, which is quite interesting as in those years there was a growth in agricultural activity. The precipitation was limited and a drier climate prevailed, which was also the case in Epidaurus Basin, except that the terrestrial inputs yield showed an oscillation pattern.

The aforementioned comparisons have implied that the hydroclimatic pattern mainly of the MCA and LIA in the Mediterranean was not uniform and showed different trends across the various basins. Specifically, the aforesaid case was determined by a combination of climatic conditions, along with important physical and geographical controls and procedures. For instance, the multicore S25_1 of Epidaurus Basin showed slightly wetter conditions during the MCA compared to the LIA. In contrast, core M2 of Athos Basin presented wetter conditions during the LIA (Gogou et al., 2016). In the same vein, analysing different proxies, a stalagmite in Kocain Cave in southern Turkey, also showed wetter conditions during the LIA and reduced precipitation during the MCA (Graham et al., 2011), while Nar Golü Lake in Turkey exhibited a reverse pattern of wet MCA and a dry LIA (Roberts et al., 2012).

Further, related to oxygenation, a 30-year (1987–2017) study of water column evolution of the oxygen and nutrient concentrations in the Epidaurus Basin has shown a succession of water oxygenation down to the bottom in the last decade of the 20th century, an oxygen decline and hypoxic conditions after the last years of the 20th century, in 1998 y CE, with a complete anoxia in 2005 y CE (Kontoyiannis et al., 2023) which are in line with the general trend of the current dataset of the core S25_1. In more detail, there is increased dissolved oxygen in the area so higher ventilation occurs. The aforesaid fact implies that there is increased water mix in the region and lower stratification.

In addition, the most important industrial, port, naval and shipbuilding facilities of the country were created on the northern shores of the Saronikos Gulf and for this additional reason it is exposed to intense anthropogenic pressure from various pollution sources, mainly in the last centuries, since it constitutes the catchment area of Athens and the port of Piraeus. Further on this, due to the considerable distance separating the Epidaurus Basin from the metropolitan area, the organic carbon distributions in the study area exhibit features akin to those found in the open sea pelagic environment. The smaller organic particles discharged from the sewage outfall linger in suspension for extended periods, undergoing a gradual decomposition process, and consequently, they fail to reach the Epidaurus Basin (Krasakopoulou et al., 2005). Further support for the assertion that the release of carbon from the treated sewage outflow does not impact the Epidaurus Basin can be found in the distribution of coprostanol content throughout the Saronikos Gulf. Two coprostanol surveys conducted in 1999 and 2007 across the entirety of Saronikos Gulf yielded results indicating the absence of sewage-derived organic material in both water particulates sediments at location S25 (Kontoyiannis et al., 2023).

Further, periods of relatively high stratification in the region, namely ca. 950, 1200, 1530, 1770 y CE), are marked by a concurrently increased tendency in the supply of terrigenous material (TerNA and TerNOH) and increased HPA values as well and they are presented well correlated with findings from the study of Gogou et al., (2016) and Luterbacher et al., (2012), in which said findings highlight the major flood events in the eastern Mediterranean and indicate wet conditions.

Finally, one more fact that should be mentioned related to the M2 (Athos Basin) and S25_1 (Epidaurus Basin) multicores is that, while SSTs patterns appear partly different; (Athos-peach) (Gogou et al., 2016), (Epidaurus-forest green), (Fig. 11), with maximum differences around the 17^{th}-18^{th} centuries, the ventilation pattern of the deep sea floor during EMTs' events appear consistent in both sites, i.e. concerning the *n*-C_{26}OH% trends (red and grey lines, respectively in Fig. 11) are very much alike. This is interesting, given the different depths of both sites, -1018 m depth for Athos and -402 m depth for Epidaurus. The Eastern Mediterranean Transient (EMT) constitutes an intermediate-to-deep Mediterranean overturning perturbation occurred in the Aegean Sea from 1988 to 1995. Furthermore, it is reported by instrumental records was likely caused by accumulation of high salinity waters in the Levantine Sea and enhanced heat loss in the Aegean Sea, in combination with surface water freshening in the Sicily Channel (Incarbona et al., 2016), reported by instrumental records. Moreover, the ACL and C_{26}OH% values are reduced during the EMTs and therefore a cooler climate and better mixing of the seabed prevailed in the study area back then. The region also shows strong seasonality (Fig. 4). Therefore, local conditions, combined with the main Aegean currents and their flow variations such as the, can cause changes in salinity/density patterns and mixing of the water layers. The aforementioned facts need more study.

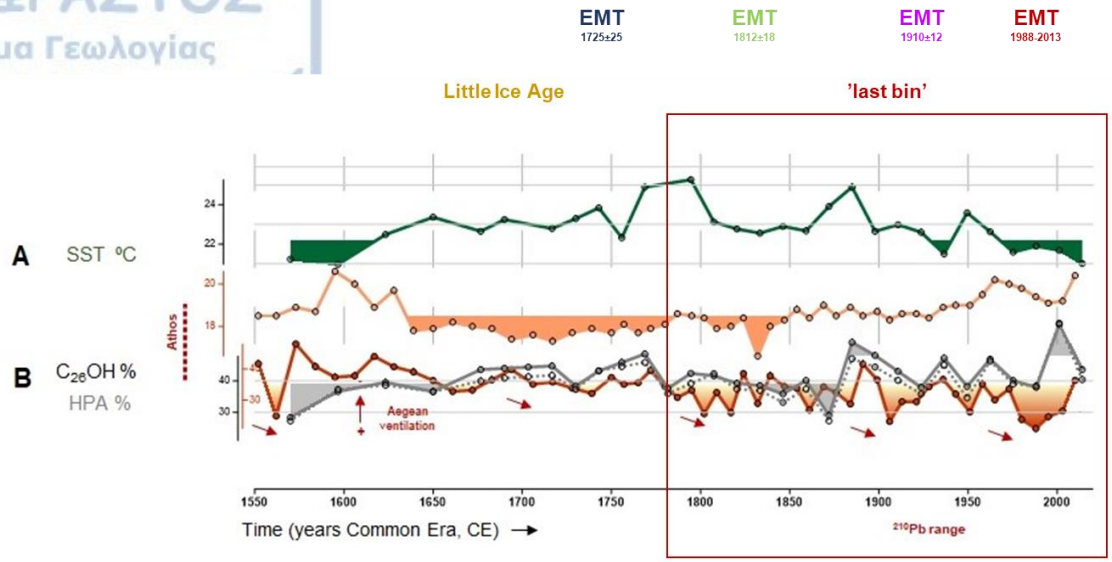

Figure 10.: Paleo-dataset in Epidaurus Basin and Athos Basin sediments over the last 1500 years. (A) Sea Surface Temperature (SST) (◦C) using alkenones, (green for Epidaurus Basin and orange for Ahos Basin) and (B) relative proportion of *n*-hexacosan-1-ol (*n*-C_{26}OH) to the sum of C_{26}OH plus *n*-C_{31} and HPA index (grey for Epidaurus Basin and red for Athos Basin). The box in red shows the time interval within the ^{210}Pb range for M2 core (Athos Basin) (Gogou et al., 2016).

6. Conclusions

6.1. Remarks

The present palaeoceanographic study is referring mainly to palaeoenvironmental reconstruction of the past 1500 years in the Epidaurus Basin, based on multi-proxy reconstructions from the sedimentary record of the S25_1 high resolution marine multi-core.

During 600-800 y CE, there was a decrease in SST until the beginning of the 8th century and drier conditions were observed, as well as there were reduced terrestrial inputs and stronger water mixing. The Late Antique Little Ice (LaLIA) onset is placed around the mid-6th century. It is described as the coldest period of the past two millennia (Büntgen et al., 2016, 2022). Given its short duration (ca. 6th-7th centuries) and the time span covered by the Epidaurus core, it is not possible to identify it unambiguously. Only SSTs are maintained below the average around the 7th-8th centuries, together with maxima for the terrestrial input and minima for the marine input at the core location. From the mid-to-late-8th century, an increase in SST and a transition from dry to wetter conditions are noted. In addition, there is an increase in all indicators and better preservation of terrestrial organic matter. This is consistent with previous studies that suggested eastern-western hydroclimate see-saws (Roberts et al., 2012). By the 9th-10th centuries, SSTs increased and oscillated around 22.2^{o}C, together with the marine Algal input, likely due to the availability of nutrients in the area receiving increasing terrestrial material. Few events of SST decreases are connected with strong supply of fresh terrestrial material, water stratification and high preservation of organic matter, as indicated by CPI_{NA} values and *n*-C_{26}OH and HPA percentages.

During the MCA period (ca. 950-1250 y CE), there is an upward trend in SST, constant values of terrestrial inputs and an increase in fresh material, while as the beginning of the 13th century is approached, a decrease in SST and drier conditions (wetter than DA and LIA) are observed.

Further, for the LIA event (ca. 13th-19th centuries CE), both marine and terrestrial inputs point to two contrasting LIA phases: a warming during the first part, around 13th-16th centuries, and a final cooling trend that culminates around the 16th-19th centuries. This would be consistent with the progressive weakening of the North Atlantic circulation, in line with the documented increased frequency of globally sustained volcanism and/or land use change (McGregor et al., 2015; Moreno-Chamarro et al., 2017). Additionally, in the Epidaurus Basin is observed that at the end of the MCA period and towards the beginning of the LIA period there is an increase in terrestrial inputs. For the LIA warming phase (ca. 1250-1500 y CE), in 1250±30 y CE, there is a trend of warming SST and an increase both in marine sterols and in the concentrations of Algal is presented which coincides with the weak water mixing revealed through the HPA index. From ca. 1320 y CE onwards a rapid decrease in SST is noticed and as we reach the beginning of the 15th century, riverine runoff increases slightly and there is a better preservation of terrestrial organic matter. Further, regarding the LIA cooling phase (ca. 1500-1850 y CE), after 1600±30 y CE the SST shows an increasing trend with the exception of a few decades, i.e. around mid and late 18th century, reasonably related to the LIA cooling phase. Still, there is an increase in the continental inputs and the concentrations of Algal, hence a greater availability of nutrients is noted. Moreover, there is a rapid increase in the UCM index

and a simultaneous decrease in the CPI_{NA} values, which reveals the beginning of the settlement of the area and the burning of wood by the people for their daily needs. From ca. 1830±30 y CE, enhanced continental inputs, rising precipitation and a degradation of organic matter, thus better water mixing is presented. Additionally, a slight transition to wetter condition is observed. In general, this interval shows a slight decrease in continental material and food availability in the marine environment. In addition, after ca. 1800±30 y CE there is better preservation of organic matter and thus better stratification of the seabed and during this period, slightly drier conditions than within the MCA are observed (average: 0.93 MCA *vs*. 0.90 LIA).

Regarding the post-industrial Era (19th century onwards), the onset of the industrial revolution around the 19th century (Abram et al., 2016) was recorded within the dating uncertainties, in the Epidaurus Basin and implied an increase in SST values of about 2^{o}C. A general alteration in all indicators appears to lead to an environmental setting receiving anthropogenic impact. This change is occurring at a much slower rate compared to other cities, as the area is far from the major urban centres of the wider region. Additionally, at the beginning of the 20th century, a trend of decreasing SST is observed and a better preservation of terrestrial organic matter in the region. The physico-chemical processes of the aforementioned fact need more study as the phenomenon of a decrease in SSTs during this period is not common. Finally, wetter conditions are presented compared to all the periods analysed and a higher nutrient availability is recorded, due to both increased terrestrial inputs and anthropogenic impact in the area.

Overall, in the Mediterranean region several studies of both marine and terrestrial records have been carried out and different variations have been noted between the various periods and different regions. A combination of different climate modes along with major physical geographical differences control climate see-saws in the region (Roberts et al., 2012).

6.2. Current study and its future perspectives

This master thesis presents some useful findings on the paleoclimatology of the Saronikos Gulf (central Aegean, northeastern Mediterranean), for the period of the last 1500 years. In particular, lipid biomarkers and their diagnostic indices have permitted the reconstruction of the SST and hydroclimatic regime during the MCA/LIA/IP intervals. Our findings showed the occurrence of wetter climatic regime during the MCA relative to the LIA and a trend of decreasing SSTs during the first decades of the 20th century. Productivity trends exhibited some interesting features regarding the terrestrial inputs and the concomitant nutrient transport to the marine environment, giving rise to marine productivity. Finally, specific biogeochemical indices of the S25_1 core when co-plotted with those reported in previous studies from the north Aegean Sea, revealed synchronous stratification *vs*. mixing processes, which pinpoint to low and high oxygenation, respectively, of the subsurface water column and the underlying sediment of the northern Aegean seabed and the Epidaurus Basin. The aforesaid facts reflect the need for further study in order to produce even more detailed climate and ocean properties' reconstructions for the whole Aegean region.

Biogeochemistry has the initial and a fundamental role in numerous environmental issues of current concern related to global change and air, water, and soil quality. Further,

biogeochemistry applied in climatology of the pastoffers quantitative and integrative analysis of coupled ocean-atmosphere-biosphere processes, useful for future climatological research.

In the current decade, assorted data repositories and database communities, such as PANGAEA, Neotoma Paleoecology Database (NEOTOMA), National Oceanic and Atmospheric Administration (NOAA), Past Global Changes (PAGES) are available and the data have been digitised and in combination with the technological development and software expansion every scientific group can revise and/or update the databases.

Regarding the Past Global Changes (PAGES) 2k databases, any scientist can access, consult and even post data. In recent years, working group teams have developed the field related to temperature and hydroclimate reconstructions and its fluctuations over the last 2000 years (Fig. 11), to help in disentangling natural from human climate changes.

Additional investigation targeting geobiological features should be a priority of future research. Seeking procedures of current and past climate and environmental conditions in different time periods will assist the competent institutions and scientists to link more data and infer even more evidence for them, especially for the regions, in which there is a lack of datasets. The cumulative biogeochemical knowledge of the current academic and professional society and the digital revolution is the ideal mixing for meritorious endeavours and notable activities to bear fruit in the immediate future, especially related to a sustainable one.

Figure 11.: (MedCLIVAR2k) Martrat et al., in prep.

7. References

Abram, N. J., McGregor, H. V., Tierney, J. E., Evans, M. N., McKay, N. P., Kaufman, D. S., Thirumalai, K., Martrat, B., Goosse, H., Phipps, S. J., Steig, E. J., Kilbourne, K. H., Saenger, C. P., Zinke, J., Leduc, G., Addison, J. A., Mortyn, P. G., Seidenkrantz, M. S., Sicre, M. A., … Von Gunten, L. (2016). Early onset of industrial-era warming across the oceans and continents. *Nature*, *536*(7617), 411–418. https://doi.org/10.1038/nature19082

Al-Khion, D. D., Al-Ali, B. S., Al-Saad, H. T., & Rushdi, A. I. (2021). Levels and source of aliphatic hydrocarbons in marine fishes from coast of Iraq Based on biomarkers and biogeochemical indices. *Indian Journal of Ecology*, *48*(2), 536–544.

Altenbach, A. V. (1992). Short term processes and patterns in the foraminiferal response to organic flux rates. *Marine Micropaleontology*, *19*(1–2), 119–129. https://doi.org/10.1016/0377-8398(92)90024-E

Appolinario, L. R., Tschoeke, D., Calegario, G., Barbosa, L. H., Moreira, M. A., Albuquerque, A. L. S., Thompson, C. C., & Thompson, F. L. (2020). Oil leakage induces changes in microbiomes of deep-sea sediments of Campos Basin (Brazil). *Science of the Total Environment*, *740*, 139556. https://doi.org/10.1016/j.scitotenv.2020.139556

Boon, J. J., Meer, F. W., Schuyl, P. J. W., Leeuw, J. W., & Schenk, P. A. (1978). *Organic geochemical analyses of core samples from site 362, Walvis Ridge, DSDP LEG 40*. *4*(1), 627–637.

Brassell, S. C., Eglinton, G., Marlowe, I. T., Pfaumann, U., & Sarnthein, M. (1986). Molecular stratigraphy : a new tool for climatic assessment. *Nature*, *320*, 129–133.

Bray, E., & Evans, E. (1961). Distribution of n-paraffins as a clue to recognition of source beds. *Geochim. Cosmochim. Acta*, *22*(1), 2–15.

Brocks, J. ., & Grice, K. (2011). *Biomarkers (Molecular Fossils)*. 147–167. https://doi.org/10.1007/978-1-4020-9212-1_30

Broerse, A. T. C., Ziveri, P., Van Hinte, J. E., & Honjo, S. (2000). Coccolithophore export production, species composition, and coccolith-CaCO3 fluxes in the NE Atlantic (34 °N 21 °W and 48 °N 21 °W). *Deep-Sea Research Part II: Topical Studies in Oceanography*, *47*(9–11), 1877–1905. https://doi.org/10.1016/S0967-0645(00)00010-2

Büntgen, U., Crivellaro, A., Arseneault, D., Baillie, M., Barclay, D., Bernabei, M., Bontadi, J., Boswijk, G., Brown, D., Christie, D. A., Churakova, O. V., Cook, E. R., D'Arrigo, R., Davi, N., Esper, J., Fonti, P., Greaves, C., Hantemirov, R. M., Hughes, M. K., … Piermattei, A. (2022). Global wood anatomical perspective on the onset of the Late Antique Little Ice Age (LALIA) in the mid-6th century CE. *Science Bulletin*, *67*(22), 2336–2344. https://doi.org/10.1016/j.scib.2022.10.019

Büntgen, U., Myglan, V. S., Ljungqvist, F. C., McCormick, M., Di Cosmo, N., Sigl, M., Jungclaus, J., Wagner, S., Krusic, P. J., Esper, J., Kaplan, J. O., De Vaan, M. A. C., Luterbacher, J., Wacker, L., Tegel, W., & Kirdyanov, A. V. (2016). Cooling and societal change during the Late Antique Little Ice Age from 536 to around 660 AD. *Nature Geoscience*, *9*(3), 231–236. https://doi.org/10.1038/ngeo2652

Cavagna, A. J., Dehairs, F., Bouillon, S., Woule-Ebongué, V., Planchon, F., Delille, B., & Bouloubassi, I. (2013). Water column distribution and carbon isotopic signal of

cholesterol, brassicasterol and particulate organic carbon in the Atlantic sector of the Southern Ocean. *Biogeosciences*, *10*(4), 2787–2801. https://doi.org/10.5194/bg-10-2787-2013

Cisneros, M., Cacho, I., Frigola, J., Canals, M., Masqué, P., Martrat, B., Casado, M., Grimalt, J. O., Pena, L. D., Margaritelli, G., & Lirer, F. (2016). Sea surface temperature variability in the central-western Mediterranean Sea during the last 2700 years: A multi-proxy and multi-record approach. *Climate of the Past*, *12*(4), 849–869. https://doi.org/10.5194/cp-12-849-2016

Consortium, P. 2k. (2017). A global multiproxy database for temperature reconstructions of the Common Era. *Scientific Data*, *4*, 170088. https://doi.org/10.1038/sdata.2017.88

Conte, M. H., Sicre, M. A., Rühlemann, C., Weber, J. C., Schulte, S., Schulz-Bull, D., & Blanz, T. (2006). Global temperature calibration of the alkenone unsaturation index (U 37k) in surface waters and comparison with surface sediments. *Geochemistry, Geophysics, Geosystems*, *7*(2). https://doi.org/10.1029/2005GC001054

Cook, B. I., Anchukaitis, K. J., Touchan, R., Meko, D. M., & Cook, E. R. (2016). Spatiotemporal drought variability in the mediterranean over the last 900 years. *Journal of Geophysical Research*, *121*(5), 2060–2074. https://doi.org/10.1002/2015JD023929

Cortés, M. ., Bollmann, J., & Thierstein, H. R. (2001). Coccolithophore ecology at the HOT station Cortés M. Y., Bollmann J. & Thierstein H. R. 2001. Coccolithophore ecology at the HOT station ALOHA, Hawaii. Deep. Res. Part II Top. Stud. Oceanogr., 48:1957–1981.ALOHA, Hawaii. *Deep-Sea Research Part II: Topical Studies in Oceanography*, *48*(8–9), 1957–1981.

Cranwell, P. A. (1972). Chain-length distribution of n-alkanes from lake sediments in relation to post-glacial environmental change. *Freshwater Biology*, *3*(3), 259–265. papers2://publication/uuid/A8180EC1-59C5-42C7-A514-6C4280EAABB7

Dachs, J., & Méjanelle, L. (2010). Organic pollutants in coastal waters, sediments, and biota: A relevant driver for ecosystems during the anthropocene? *Estuaries and Coasts*, *33*(1), 1–14. https://doi.org/10.1007/s12237-009-9255-8

Dobrovolný, P., Moberg, A., Brázdil, R., Pfister, C., Glaser, R., Wilson, R., van Engelen, A., Limanówka, D., Kiss, A., Halíčková, M., Macková, J., Riemann, D., Luterbacher, J., & Böhm, R. (2010). Monthly, seasonal and annual temperature reconstructions for Central Europe derived from documentary evidence and instrumental records since AD 1500. *Climatic Change*, *101*(1), 69–107. https://doi.org/10.1007/s10584-009-9724-x

Drăguşin, V., Staubwasser, M., Hoffmann, D. L., Ersek, V., Onac, B. P., & Veres, D. (2014). Constraining Holocene hydrological changes in the Carpathian-Balkan region using speleothem δ18O and pollen-based temperature reconstructions. *Climate of the Past*, *10*(4), 1363–1380. https://doi.org/10.5194/cp-10-1363-2014

Drakatos, G., Karastathis, V., Makris, J., Papoulia, J., & Stavrakakis, G. (2005). 3D crustal structure in the neotectonic basin of the Gulf of Saronikos (Greece). *Tectonophysics*, *400*(1–4), 55–65. https://doi.org/10.1016/j.tecto.2005.02.004

Duan Fengkui, F., He, K., & Liu, X. (2010). Characteristics and source identification of fine particulate n-alkanes in Beijing, China. *Journal of Environmental Sciences*, *22*(7), 998–1005. https://doi.org/10.1016/S1001-0742(09)60210-2

Eglinton, G., & Hamilton, R. J. (1967). Leaf epicuticular waxes : The waxy outer surfaces of

most plants display a wide diversity of fine structure and chemical constituents. *Science*, *156*(3780), 1322–1335.

Esper, J., Frank, D., Büntgen, U., Verstege, A., Luterbacher, J., & Xoplaki, E. (2007). Long-term drought severity variations in Morocco. *Geophysical Research Letters*, *34*(17), 1–5. https://doi.org/10.1029/2007GL030844

Facorellis, Y., & Vardala-Theodorou, E. (2015). Sea Surface Radiocarbon Reservoir Age Changes in the Aegean Sea from about 11,200 BP to Present. *Radiocarbon*, *57*(3), 493–505. https://doi.org/10.2458/azu_rc.57.18363

Felis, T., Pätzold, J., Loya, Y., Fine, M., Nawar, A. H., & Wefer, G. (2000). A coral oxygen isotope record from the northern Red Sea documenting NAO, ENSO, and North Pacific teleconnections on Middle East climate variability since the year 1750. *Paleoceanography*, *15*(6), 679–694. https://doi.org/10.1029/1999PA000477

Foutrakis, P. M., & Anastasakis, G. (2020). Quaternary continental shelf basins of Saronikos Gulf, Aegean Sea. *Geo-Marine Letters*, *40*(5), 629–647. https://doi.org/10.1007/s00367-020-00653-9

Friligos, N. (1983). Enrichment of inorganic nutrients in the Western Saronikos Gulf. *Marine Pollution Bulletin*, *14*(2), 52–57. https://doi.org/10.1016/0025-326X(83)90191-1

Gelin, F., Boogers, I., Noordeloos, A. A. M., Sinninghe Damsté, J. S., Riegman, R., & De Leeuw, J. W. (1997). Resistant biomacromolecules in marine microalgae of the classes eustigmatophyceae and chlorophyceae: Geochemical implications. *Organic Geochemistry*, *26*(11–12), 659–675. https://doi.org/10.1016/S0146-6380(97)00035-1

Gibbard, P. L., Bauer, A. M., Edgeworth, M., Ruddiman, W. F., Gill, J. L., Merritts, D. J., Finney, S. C., Edwards, L. E., Walker, M. . C., Maslin, M., & Ellis, E. C. (2022). A practical solution: the Anthropocene is a geological event, not a formal epoch. *Episodes*, *45*(4), 349–357. https://doi.org/10.18814/epiiugs/2021/021029

Gogou, A., Bouloubassi, I., Lykousis, V., Arnaboldi, M., Gaitani, P., & Meyers, P. A. (2007). Organic geochemical evidence of Late Glacial-Holocene climate instability in the North Aegean Sea. *Palaeogeography, Palaeoclimatology, Palaeoecology*, *256*(1–2), 1–20. https://doi.org/10.1016/j.palaeo.2007.08.002

Gogou, A., Bouloubassi, I., & Stephanou, E. G. (2000). Marine organic geochemistry of the Eastern Mediterranean: 1. Aliphatic and polyaromatic hydrocarbons in Cretan Sea surficial sediments. *Marine Chemistry*, *68*(4), 265–282. https://doi.org/10.1016/S0304-4203(99)00082-1

Gogou, A., Triantaphyllou, M., Xoplaki, E., Izdebski, A., Parinos, C., Dimiza, M., Bouloubassi, I., Luterbacher, J., Kouli, K., Martrat, B., Toreti, A., Fleitmann, D., Rousakis, G., Kaberi, H., Athanasiou, M., & Lykousis, V. (2016). Climate variability and socio-environmental changes in the northern Aegean (NE Mediterranean) during the last 1500 years. *Quaternary Science Reviews*, *136*, 209–228. https://doi.org/10.1016/j.quascirev.2016.01.009

Gough, M. A., & Rowland, S. J. (1990). Characterization of unresolved complex mixtures of hydrocarbons in petroleum. In *Nature* (Vol. 344, Issue 6267, pp. 648–650). https://doi.org/10.1038/344648a0

Graham, N. E., Ammann, C. M., Fleitmann, D., Cobb, K. M., & Luterbacher, J. (2011). Support for global climate reorganization during the "Medieval Climate Anomaly." *Climate*

Dynamics, *37*(5), 1217–1245. https://doi.org/10.1007/s00382-010-0914-z

Grice, K., Klein Breteler, W. C. M., Schouten, S., Grossi, V., De Leeuw, J. W., & Sinninghe Damsté, J. S. (1998). Effects of zooplankton herbivory on biomarker proxy records. *Paleoceanography*, *13*(6), 686–693. https://doi.org/10.1029/98PA01871

Harada, N., Handa, N., Harada, K., & Matsuoka, H. (2001). Alkenones and particulate fluxes in sediment traps from the central equatorial Pacific. *Deep-Sea Research Part I: Oceanographic Research Papers*, *48*(3), 891–907. https://doi.org/10.1016/S0967-0637(00)00077-7

Hasanuzzaman, M., Ueno, A., Ito, H., Ito, Y., Yamamoto, Y., Yumoto, I., & Okuyama, H. (2007). Degradation of long-chain n-alkanes (C36 and C40) by Pseudomonas aeruginosa strain WatG. *International Biodeterioration and Biodegradation*, *59*(1), 40–43. https://doi.org/10.1016/j.ibiod.2006.07.010

Hays, M. D., Smith, N. D., & Dong, Y. (2004). Nature of unresolved complex mixture in size-distributed emissions from residential wood combustion as measured by thermal desorption-gas chromatography-mass spectrometry. *Journal of Geophysical Research D: Atmospheres*, *109*(16), 1–13. https://doi.org/10.1029/2003JD004051

Herbert, T. D. (2003). Alkenone Paleotemperature Determinations. *Treatise on Geochemistry*, *6–9*, 391–432. https://doi.org/10.1016/B0-08-043751-6/06115-6

Hernández, A., Martin-Puertas, C., Moffa-Sánchez, P., Moreno-Chamarro, E., Ortega, P., Blockley, S., Cobb, K. M., Comas-Bru, L., Giralt, S., Goosse, H., Luterbacher, J., Martrat, B., Muscheler, R., Parnell, A., Pla-Rabes, S., Sjolte, J., Scaife, A. A., Swingedouw, D., Wise, E., & Xu, G. (2020). Modes of climate variability: Synthesis and review of proxy-based reconstructions through the Holocene. *Earth-Science Reviews*, *209*(December 2019), 103286. https://doi.org/10.1016/j.earscirev.2020.103286

Huang, Y., Dupont, L., Sarnthein, M., Hayes, J. M., & Eglinton, G. (2000). Mapping of C4 plant input from North West Africa into North East Atlantic sediments. *Geochimica et Cosmochimica Acta*, *64*(20), 3505–3513. https://doi.org/10.1016/S0016-7037(00)00445-2

Hudson, E. D., Parrish, C. C., & Helleur, R. J. (2001). Biogeochemistry of sterols in plankton, settling particles and recent sediments in a cold ocean ecosystem (Trinity Bay, Newfoundland). *Marine Chemistry*, *76*(4), 253–270. https://doi.org/10.1016/S0304-4203(01)00066-4

Huguet, C., Kim, J. H., González-Arango, C., Ramírez-Valencia, V., Kang, S., Gal, J. K., & Shin, K. H. (2019). Sources of organic matter in two contrasting tropical coastal environments: The Caribbean Sea and the eastern Pacific. *Journal of South American Earth Sciences*, *96*(September). https://doi.org/10.1016/j.jsames.2019.102349

Hurrell, J. W., Kushnir, Y., Ottersen, G., & Visbeck, M. (2003). An overview of the north atlantic oscillation. *Geophysical Monograph Series*, *134*, 1–35. https://doi.org/10.1029/134GM01

Incarbona, A., Abu-Zied, R. H., Rohling, E. J., & Ziveri, P. (2019). Reventilation Episodes During the Sapropel S1 Deposition in the Eastern Mediterranean Based on Holococcolith Preservation. *Paleoceanography and Paleoclimatology*, *34*(10), 1597–1609. https://doi.org/10.1029/2019PA003626

Incarbona, A., Martrat, B., Mortyn, P. G., Sprovieri, M., Ziveri, P., Gogou, A., Jordà, G., Xoplaki,

E., Luterbacher, J., Langone, L., Marino, G., Rodríguez-Sanz, L., Triantaphyllou, M., Di Stefano, E., Grimalt, J. O., Tranchida, G., Sprovieri, R., & Mazzola, S. (2016). Mediterranean circulation perturbations over the last five centuries: Relevance to past Eastern Mediterranean Transient-type events. *Scientific Reports*, *6*(January). https://doi.org/10.1038/srep29623

Isoe, S., Hyeon, S. B., Katsumura, S., & Sakan, T. (1972). Photo-oxygenation of carotenoids. II. The absolute configuration of loliolide and dihydroactinidiolide. *Tetrahedron Letters*, *13*(25), 2517–2520. https://doi.org/10.1016/S0040-4039(01)84863-2

Jalali, B., Sicre, M. A., Klein, V., Schmidt, S., Maselli, V., Lirer, F., Bassetti, M. A., Toucanne, S., Jorry, S. J., Insinga, D. ., Petrosino, P., & Châles, F. (2018). Deltaic and Coastal Sediments as Recorders of Mediterranean Regional Climate and Human Impact Over the Past Three Millennia. *Paleoceanography and Paleoclimatology*, *33*(6), 579–593. https://doi.org/10.1029/2017PA003298

Jones, P. D., Osborn, T. J., & Briffa, K. R. (2001). The evolution of climate over the last millennium. *Science*, *292*(5517), 662–667. https://doi.org/10.1126/science.1059126

Klok, J., Baas, M., Cox, H. C., de Leeuw, J. W., & Schenck, P. A. (1984). Loliolides and dihydroactinidiolide in a recent marine sediment probably indicate a major transformation pathway of carotenoids. *Tetrahedron Letters*, *25*(48), 5577–5580. https://doi.org/10.1016/S0040-4039(01)81631-2

Konecky, B. L., McKay, N. P., Churakova, O. V., Comas-Bru, L., Dassié, E. P., DeLong, K. L., Falster, G. M., Fischer, M. J., Jones, M. D., Jonkers, L., Kaufman, D. S., Leduc, G., Managave, S. R., Martrat, B., Opel, T., Orsi, A. J., Partin, J. W., Sayani, H. R., Thomas, E. K., … Yoshimura, K. (2020). The Iso2k database: A global compilation of paleo-δ18O and δ2H records to aid understanding of Common Era climate. *Earth System Science Data*, *12*(3), 2261–2288. https://doi.org/10.5194/essd-12-2261-2020

Kontoyiannis, H. (2010). Observations on the circulation of the Saronikos Gulf: A Mediterranean embayment sea border of Athens, Greece. *Journal of Geophysical Research: Oceans*, *115*(6), 1–23. https://doi.org/10.1029/2008JC005026

Kontoyiannis, H., Pavlidou, A., Zeri, C., Krasakopoulou, E., Simboura, N., Hatzianestis, I., Papadopoulos, V. P., Rousselaki, E., Asimakopoulou, G., & Siokou, I. (2023). *Science of the Total Environment Thirty years of a bottom oxygen depletion-renewal cycle in the coastal yet deep environment of the West Saronikos Gulf (Greece): Its drivers and the impact on the benthic communities*. *902*(June).

Kouli, K., Gogou, A., Bouloubassi, I., Triantaphyllou, M. V., Ioakim, C., Katsouras, G., Roussakis, G., & Lykousis, V. (2012). Late postglacial paleoenvironmental change in the northeastern Mediterranean region: Combined palynological and molecular biomarker evidence. *Quaternary International*, *261*, 118–127. https://doi.org/10.1016/j.quaint.2011.10.036

Lolis, C. J., Bartzokas, A., & Katsoulis, B. D. (2002). Spatial and temporal 850 hPa air temperature and sea-surface temperature covariances in the Mediterranean region and their connection to atmospheric circulation. *International Journal of Climatology*, *22*(6), 663–676. https://doi.org/10.1002/joc.759

Luo, G., Yang, H., Algeo, T. J., Hallmann, C., & Xie, S. (2018). Lipid biomarkers for the reconstruction of deep-time environmental conditions. *Earth-Science Reviews*, *189*, 99–124. https://doi.org/10.1016/j.earscirev.2018.03.005

Luterbacher, J., García-Herrera, R., Akcer-On, S., Allan, R., Alvarez-Castro, M. C., Benito, G., Booth, J., Büntgen, U., Cagatay, N., Colombaroli, D., Davis, B., Esper, J., Felis, T., Fleitmann, D., Frank, D., Gallego, D., Garcia-Bustamante, E., Glaser, R., Gonzalez-Rouco, F. J., … Zorita, E. (2012). A Review of 2000 Years of Paleoclimatic Evidence in the Mediterranean. In *The Climate of the Mediterranean Region: From the Past to the Future* (Issue November). https://doi.org/10.1016/B978-0-12-416042-2.00002-1

Mahairas, P., & Balafoutis, C. (1997). *General Climatology with Meteorology elements*. UNIVERSITY STUDIO PRESS.

Malinverno, E., Triantaphyllou, M. V., Stavrakakis, S., Ziveri, P., & Lykousis, V. (2009). Seasonal and spatial variability of coccolithophore export production at the South-Western margin of Crete (Eastern Mediterranean). *Marine Micropaleontology*, *71*(3–4), 131–147. https://doi.org/10.1016/j.marmicro.2009.02.002

Marlowe, I. T., Green, J. C., Neal, A. C., Brassell, S. C., & Course, P. A. (1984). Long chain (n-C37-C39) alkenones in the Prymnesiophyceae. Distribution of lkenones and other lipids and their taxonomic significance. *British Phycological Journal*, *19*(September 1), 37–41.

Martín-Chivelet, J., Muñoz-García, M. B., Edwards, R. L., Turrero, M. J., & Ortega, A. (2011). Land surface temperature changes in Northern Iberia since 4000yrBP, based on δ13C of speleothems. *Global and Planetary Change*, *77*(1–2), 1–12. https://doi.org/10.1016/j.gloplacha.2011.02.002

Martín-Puertas, C., Jiménez-Espejo, F., Martínez-Ruiz, F., Nieto-Moreno, V., Rodrigo, M., Mata, M. P., & Valero-Garcés, B. L. (2010). Late Holocene climate variability in the southwestern Mediterranean region: An integrated marine and terrestrial geochemical approach. *Climate of the Past*, *6*(6), 807–816. https://doi.org/10.5194/cp-6-807-2010

Martrat, B., Grimalt, J. O., Shackleton, N. J., de Abreu, L., Hutterli, M. A., & Stocker, T. F. (2007). Four Climate Cycles of Recurring Deep and Surface Water Destabilizations on the Iberian Margin. *Science*, *317*(July), 502–507. https://doi.org/10.1126/science.113999

Marullo, S., Artale, V., & Santoleri, R. (2011). The SST multidecadal variability in the Atlantic-Mediterranean region and its relation to AMO. *Journal of Climate*, *24*(16), 4385–4401. https://doi.org/10.1175/2011JCLI3884.1

Matiatos, I. (2010). *Isotope hydrology study of areas in Argolis Peninsula* [National and Kapodistrian University of Athens]. https://thesis.ekt.gr/thesisBookReader/id/24160?lang=el#page/1/mode/2up

McGregor, H. V., Evans, M. N., Goosse, H., Leduc, G., Martrat, B., Addison, J. A., Mortyn, P. G., Oppo, D. W., Seidenkrantz, M. S., Sicre, M. A., Phipps, S. J., Selvaraj, K., Thirumalai, K., Filipsson, H. L., & Ersek, V. (2015). Robust global ocean cooling trend for the pre-industrial Common Era. *Nature Geoscience*, *8*(9), 671–677. https://doi.org/10.1038/ngeo2510

Menzel, D., Van Bergen, P. F., Schouten, S., & Sinninghe Damsté, J. S. (2003). Reconstruction of changes in export productivity during Pliocene sapropel deposition: A biomarker approach. *Palaeogeography, Palaeoclimatology, Palaeoecology*, *190*, 273–287. https://doi.org/10.1016/S0031-0182(02)00610-7

Michelakaki, M., & Kitsiou, D. (2005). Estimation of Anisotropies in Chlorophyll A spatial distributions based on satellite data and variography. *Global NEST JournalGlobal NEST: The International Journal*, *7*(2), 204–211. https://doi.org/10.30955/gnj.000361

Moldoveanu, S. C., & David, V. (2019). Derivatization Methods in GC and GC/MS. *Gas Chromatography - Derivatization, Sample Preparation, Application*, 1–33. https://doi.org/10.5772/intechopen.81954

Moreno-Chamarro, E., Zanchettin, D., Lohmann, K., Luterbacher, J., & Jungclaus, J. H. (2017). Winter amplification of the European Little Ice Age cooling by the subpolar gyre. *Scientific Reports*, *7*(1), 1–8. https://doi.org/10.1038/s41598-017-07969-0

Mouradian, M., Panetta, R. J., De Vernal, A., & Gélinas, Y. (2007). Dinosterols or dinocysts to estimate dinoflagellate contributions to marine sedimentary organic matter? *Limnology and Oceanography*, *52*(6), 2569–2581. https://doi.org/10.4319/lo.2007.52.6.2569

Müller, P. J., Kirst, G., Ruhland, G., Von Storch, I., & Rosell-Melé, A. (1998). Calibration of the alkenone paleotemperature index U37K based on core-tops from the eastern South Atlantic and the global ocean (60°N-60°S). *Geochimica et Cosmochimica Acta*, *62*(10), 1757–1772. https://doi.org/10.1016/S0016-7037(98)00097-0

Nash, D., Leeming, R., Clemow, L., Hannah, M., Halliwell, D., & Allen, D. (2005). Quantitative determination of sterols and other alcohols in overland flow from grazing land and possible source materials. *Water Research*, *39*(13), 2964–2978. https://doi.org/10.1016/j.watres.2005.04.063

Nieto-Moreno, V., Martinez-Ruiz, F., Giralt, S., Gallego-Torres, D., García-Orellana, J., Masqué, P., & Ortega-Huertas, M. (2013). Climate imprints during the "Medieval Climate Anomaly" and the "Little Ice Age" in marine records from the Alboran Sea basin. *Holocene*, *23*(9), 1227–1237. https://doi.org/10.1177/0959683613484613

Ohkouchi, N., Kawamura, K., Kawahata, H., & Taira, A. (1997). Latitudinal distributions of terrestrial biomarkers in the sediments from the Central Pacific. *Geochimica et Cosmochimica Acta*, *61*(9), 1911–1918. https://doi.org/10.1016/S0016-7037(97)00040-9

Ouyang, X., Guo, F., & Bu, H. (2015). Lipid biomarkers and pertinent indices from aquatic environment record paleoclimate and paleoenvironment changes. *Quaternary Science Reviews*, *123*, 180–192. https://doi.org/10.1016/j.quascirev.2015.06.029

Pallacks, S., Ziveri, P., Martrat, B., Mortyn, P. G., Grelaud, M., Schiebel, R., Incarbona, A., Garcia-Orellana, J., & Anglada-Ortiz, G. (2021). Planktic foraminiferal changes in the western Mediterranean Anthropocene. *Global and Planetary Change*, *204*, 103549. https://doi.org/10.1016/j.gloplacha.2021.103549

Papanikolaou, D., & Sideris, C. I. (2014). *Geology* (7th ed.). Patakis.

Parinos, C., Gogou, A., Bouloubassi, I., Pedrosa-Pàmies, R., Hatzianestis, I., Sanchez-Vidal, A., Rousakis, G., Velaoras, D., Krokos, G., & Lykousis, V. (2013). Occurrence, sources and transport pathways of natural and anthropogenic hydrocarbons in deep-sea sediments of the eastern Mediterranean Sea. *Biogeosciences*, *10*(9), 6069–6089. https://doi.org/10.5194/bg-10-6069-2013

Pedrosa-Pàmies, R., Conte, M. H., Weber, J. C., & Johnson, R. (2018). Carbon cycling in the Sargasso Sea water column: Insights from lipid biomarkers in suspended particles. *Progress in Oceanography*, *168*, 248–278. https://doi.org/10.1016/j.pocean.2018.08.005

Pedrosa-Pàmies, R., Conte, M. H., Weber, J. C., & Johnson, R. (2019). Hurricanes Enhance Labile Carbon Export to the Deep Ocean. *Geophysical Research Letters*, *46*(17–18), 10484–10494. https://doi.org/10.1029/2019GL083719

Pedrosa-Pàmies, R., Parinos, C., Sanchez-Vidal, A., Gogou, A., Calafat, A., Canals, M.,

Bouloubassi, I., & Lampadariou, N. (2015). Composition and sources of sedimentary organic matter in the deep eastern Mediterranean Sea. *Biogeosciences*, *12*(24), 7379–7402. https://doi.org/10.5194/bg-12-7379-2015

Peel, M. C., Finlayson, B. L., & McMahon, T. A. (2007). Updated world map of the Köppen-Geiger climate classification. *Hydrol. Earth Syst.*, *11*(5), 1633–1644. https://doi.org/10.5194/hess-11-1633-2007

Percot, A., Yalçin, A., Aysel, V., Erduğan, H., Dural, B., & Güven, K. C. (2009). Loliolide in marine algae. *Natural Product Research*, *23*(5), 460–465. https://doi.org/10.1080/14786410802076069

Poynter, J., & Eglinton, G. (1990). Molecular composition of three sediments from hole 717C: the Bengal Fan. *Proc., Scientific Results, ODP, Leg 116, Distal Bengal Fan*, *116*, 155–161. https://doi.org/10.2973/odp.proc.sr.116.151.1990

Prahl, F. G., Muehlhausen, L. A., & Zahnle, D. L. (1988). Further evaluation of long-chain alkenones as indicators of paleoceanographic conditions. *Geochimica et Cosmochimica Acta*, *52*(9), 2303–2310. https://doi.org/10.1016/0016-7037(88)90132-9

Prahl, F. G., & Wakeham, S. G. (1987). Calibration of unsaturation patterns in long-chain ketone compositions for palaeotemperature assessment. *Nature*, *330*(6146), 367–369. https://doi.org/10.1038/330367a0

Rampen, S. W., Schouten, S., Koning, E., Brummer, G. J. A., & Sinninghe Damsté, J. S. (2008). A 90 kyr upwelling record from the northwestern Indian Ocean using a novel long-chain diol index. *Earth and Planetary Science Letters*, *276*(1–2), 207–213. https://doi.org/10.1016/j.epsl.2008.09.022

Rampen, S. W., Willmott, V., Kim, J. H., Uliana, E., Mollenhauer, G., Schefuß, E., Sinninghe Damsté, J. S., & Schouten, S. (2012). Long chain 1,13- and 1,15-diols as a potential proxy for palaeotemperature reconstruction. *Geochimica et Cosmochimica Acta*, *84*, 204–216. https://doi.org/10.1016/j.gca.2012.01.024

Reimer, P. J., Bard, E., Bayliss, A., Beck, J. W., Blackwell, P. G., Ramsey, C. B., Buck, C. E., Cheng, H., Edwards, R. L., Friedrich, M., Grootes, P. M., Guilderson, T. P., Haflidason, H., Hajdas, I., Hatté, C., Heaton, T. J., Hoffmann, D. L., Hogg, A. G., Hughen, K. A., … van der Plicht, J. (2013). IntCal13 and Marine13 Radiocarbon Age Calibration Curves 0–50,000 Years cal BP. *Radiocarbon*, *55*(4), 1869–1887. https://doi.org/10.2458/azu_js_rc.55.16947

Repeta, D. J. (1989). Carotenoid diagenesis in recent marine sediments: II. Degradation of fucoxanthin to loliolide. *Geochimica et Cosmochimica Acta*, *53*(3), 699–707. https://doi.org/10.1016/0016-7037(89)90012-4

Roberts, N., Moreno, A., Valero-Garcés, B. L., Corella, J. P., Jones, M., Allcock, S., Woodbridge, J., Morellón, M., Luterbacher, J., Xoplaki, E., & Türkeş, M. (2012). Palaeolimnological evidence for an east-west climate see-saw in the Mediterranean since AD 900. *Global and Planetary Change*, *84–85*, 23–34. https://doi.org/10.1016/j.gloplacha.2011.11.002

Robinson, A. R., Malanotte-Rizzoli, P., Hecht, A., Michelato, A., Roether, W., Theocharis, A., Ünlüata, Ü., Artegiani, A., Bergamasco, A., Bishop, J., Brenner, S., Christianidis, S., Gacic, M., Georgopoulos, D., Golnaraghi, M., Hausmann, M., Junghaus, H. G., Lascaratos, A., Latif, M. A., … Osman, M. (1992). General circulation of the Eastern Mediterranean. *Earth Science Reviews*, *32*(4), 285–309. https://doi.org/10.1016/0012-8252(92)90002-B

Rodrigo-Gámiz, M., Martínez-Ruiz, F., Rampen, S. W., Schouten, S., & Sinninghe Damsté, J. S. (2013). *Sea surface temperature variations in the western Mediterranean Sea over the last 20 kyr: A dual-organic proxy (UK'37 and LDI) approach*. 87–98. https://doi.org/10.1002/2013PA002466.Received

Rohling, E. J. (1994). Review and new aspects concerning the formation of eastern Mediterranean sapropels. *Marine Geology*, *122*(1–2), 1–28. https://doi.org/10.1016/0025-3227(94)90202-X

Rohling, E. J., Marino, G., & Grant, K. M. (2015). Mediterranean climate and oceanography, and the periodic development of anoxic events (sapropels). *Earth-Science Reviews*, *143*, 62–97. https://doi.org/10.1016/j.earscirev.2015.01.008

Rosell-Melé, A., & McClymont, E. L. (2007). Biomarkers as Paleoceanographic Proxies. *Developments in Marine Geology*, *1*(07), 441–490. https://doi.org/10.1016/S1572-5480(07)01016-0

Rushdi, A. I., Douabul, A. ., Mohammed, S. S., & Simoneit, B. R. T. (2006). Compositions and sources of extractable organic matter in Mesopotamian marshland surface sediments of Iraq. I: Aliphatic lipids. *Environmental Geology*, *50*(6), 857–866. https://doi.org/10.1007/s00254-006-0257-6

Rushdi, A. I., DouAbul, A. A. Z., Al-Maarofi, S. S., & Simoneit, B. R. T. (2018). Impacts of Mesopotamian wetland re-flooding on the lipid biomarker distributions in sediments. *Journal of Hydrology*, *558*, 20–28. https://doi.org/10.1016/j.jhydrol.2018.01.030

Sargent, J. R., & Gatten, R. R. (1974). *The distribution and metabolism of wax esters in marine invertebrates*. *4*(April 1976), 9–11.

Sawada, K., Handa, N., Shiraiwa, Y., Danbara, A., & Montani, S. (1996). Long-chain alkenones and alkyl alkenoates in the coastal and pelagic sediments of the northwest north Pacific, with special reference to the reconstruction of Emiliania huxleyi and Gephyrocapsa oceanica ratios. *Organic Geochemistry*, *24*(8–9), 751–764. https://doi.org/10.1016/S0146-6380(96)00087-3

Scarlett, A., Galloway, T. S., & Rowland, S. J. (2007). Chronic toxicity of unresolved complex mixtures (UCM) of hydrocarbons in marine sediments. *Journal of Soils and Sediments*, *7*(4), 200–206. https://doi.org/10.1065/jss2007.06.232

Sicre, M. A., Jalali, B., Martrat, B., Schmidt, S., Bassetti, M. A., & Kallel, N. (2016). Sea surface temperature variability in the North Western Mediterranean Sea (Gulf of Lion) during the Common Era. *Earth and Planetary Science Letters*, *456*, 124–133. https://doi.org/10.1016/j.epsl.2016.09.032

Sikes, E. L., Volkman, J. K., Robertson, L. G., & Pichon, J. J. (1997). Alkenones and alkenes in surface waters and sediments of the Southern Ocean: Implications for paleotemperature estimation in polar regions. *Geochimica et Cosmochimica Acta*, *61*(7), 1495–1505. https://doi.org/10.1016/S0016-7037(97)00017-3

Simoneit, B. R. T. (1984). Organic matter of the troposphere-III. Characterization and sources of petroleum and pyrogenic residues in aerosols over the western united states. *Atmospheric Environment (1967)*, *18*(1), 51–67. https://doi.org/10.1016/0004-6981(84)90228-2

Sprengel, C., Baumann, K. H., & Neuer, S. (2000). Seasonal and interannual variation of coccolithophore fluxes and species composition in sediment traps north of Gran Canaria

(29 °N 15 °W). *Marine Micropaleontology*, *39*(1–4), 157–178. https://doi.org/10.1016/S0377-8398(00)00019-0

Strong, D., Flecker, R., Valdes, P. J., Wilkinson, I. P., Rees, J. G., Michaelides, K., Zong, Y. Q., Lloyd, J. M., Yu, F. L., & Pancost, R. D. (2013). A new regional, mid-Holocene palaeoprecipitation signal of the Asian Summer Monsoon. *Quaternary Science Reviews*, *78*, 65–76. https://doi.org/10.1016/j.quascirev.2013.07.034

Theocharis, A., Georgopoulos, D., Lascaratos, A., & Nittis, K. (1993). Water masses and circulation in the central region of the Eastern Mediterranean. *Deep-Sea Research II*, *40*(6), 1121–1142.

Tierney, J. E., & Tingley, M. P. (2018). BAYSPLINE: A New Calibration for the Alkenone Paleothermometer. *Paleoceanography and Paleoclimatology*, *33*(3), 281–301. https://doi.org/10.1002/2017PA003201

Triantaphyllou, M., & Dimiza, M. (2012). *Micropalaeontology and Geoenvironment*. ION Publishing Group.

Triantaphyllou, M., Gogou, A., Dimiza, M., Kostopoulou, S., Parinos, C., Roussakis, G., Geraga, M., Bouloubassi, I., Fleitmann, D., Zervakis, V., Velaoras, D., Diamantopoulou, A., Sampatakaki, A., & Lykousis, V. (2016). Holocene Climatic Optimum centennial-scale paleoceanography in the NE Aegean (Mediterranean Sea). *Geo-Marine Letters*, *36*(1), 51–66. https://doi.org/10.1007/s00367-015-0426-2

Triantaphyllou, M. V., Baumann, K. H., Karatsolis, B. T., Dimiza, M. D., Psarra, S., Skampa, E., Patoucheas, P., Vollmar, N. M., Koukousioura, O., Katsigera, A., Krasakopoulou, E., & Nomikou, P. (2018). Coccolithophore community response along a natural CO2 gradient off Methana (SW Saronikos Gulf, Greece, NE Mediterranean). *PLoS ONE*, *13*(7). https://doi.org/10.1371/journal.pone.0200012

Triantaphyllou, M., Ziveri, P., Gogou, A., Marino, G., Lykousis, V., Bouloubassi, I., Emeis, K. C., Kouli, K., Dimiza, M., Rosell-Melé, A., Papanikolaou, M., Katsouras, G., & Nunez, N. (2009). Late Glacial-Holocene climate variability at the south-eastern margin of the Aegean Sea. *Marine Geology*, *266*(1–4), 182–197. https://doi.org/10.1016/j.margeo.2009.08.005

Tselepides, A., Zervakis, V., Polychronaki, T., Danovaro, R., & Chronis, G. (2000). Distribution of nutrients and particulate organic matter in relation to the prevailing hydrographic features of the Cretan Sea (NE Mediterrarean). *Progress in Oceanography*, *46*(2–4), 113–142. https://doi.org/10.1016/S0079-6611(00)00015-X

Tyson, R. (2006). The Biomarker Guide. Volume 1: Biomarkers and Isotopes in the Environment and Human History. Volume 2: Biomarkers and Isotopes in Petroleum Exploration and Earth History . Second Edition. (First. *Geological Magazine*, *143*(2), 249–250. https://doi.org/10.1017/s0016756806212056

Tzanis, A., Efstathiou, A., Chailas, S., & Stamatakis, M. (2018). Evidence of recent plutonic magmatism beneath Northeast Peloponnesus (Greece) and its relationship to regional tectonics. *Geophysical Journal International*, *212*(3), 1600–1626. https://doi.org/10.1093/gji/ggx486

Van der Meer, M. T. J., Benthien, A., Bijma, J., Schouten, S., & Sinninghe Damsté, J. S. (2013). Alkenone distribution impacts the hydrogen isotopic composition of the C37:2 and C37:3 alkan-2-ones in emiliania huxleyi. *Geochimica et Cosmochimica Acta*, *111*, 162–166. https://doi.org/10.1016/j.gca.2012.10.041

Velaoras, D., Zervakis, V., & Theocharis, A. (2021). *The Physical Characteristics and Dynamics of the Aegean Water Masses*. https://doi.org/10.1007/698_2020_730

Versteegh, G. J. M. (2005). Solar forcing of climate. 2: Evidence from the past. *Space Science Reviews*, *120*(3–4), 243–286. https://doi.org/10.1007/s11214-005-7047-4

Versteegh, G. J. M., Jansen, J. H. F., De Leeuw, J. W., & Schneider, R. R. (2000). Mid-chain diols and keto-ols in SE Atlantic sediments: A new tool for tracing past sea surface water masses? *Geochimica et Cosmochimica Acta*, *64*(11), 1879–1892. https://doi.org/10.1016/S0016-7037(99)00398-1

Versteegh, G. J. M., & Lipp, J. (2019). Detection of new long-chain mid-chain keto-ol isomers from marine sediments by means of HPLC–APCI-MS and comparison with long-chain mid-chain diols from the same samples. *Organic Geochemistry*, *133*, 92–102. https://doi.org/10.1016/j.orggeochem.2019.04.004

Volkman, J. K. (1986). A review of sterol markers for marine and terrigenous organic matter. *Organic Geochemistry*, *9*(2), 83–99. https://doi.org/10.1016/0146-6380(86)90089-6

Volkman, J. K. (2003). Sterols in microorganisms. *Applied Microbiology and Biotechnology*, *60*(5), 495–506. https://doi.org/10.1007/s00253-002-1172-8

Volkman, J. K. (2005). Sterols and other triterpenoids: Source specificity and evolution of biosynthetic pathways. *Organic Geochemistry*, *36*(2), 139–159. https://doi.org/10.1016/j.orggeochem.2004.06.013

Volkman, J. K., Barrett, S. M., & Blackburn, S. I. (1999). Eustigmatophyte microalgae are potential sources of C29 sterols, C22-C28 n-alcohols and C28-C32 n-alkyl diols in freshwater environments. *Organic Geochemistry*, *30*(5), 307–318. https://doi.org/10.1016/S0146-6380(99)00009-1

Volkman, J. K., Barrett, S. M., Blackburn, S. I., & Sikes, E. L. (1995). Alkenones in Gephyrocapsa oceanica: Implications for studies in paleoclimate. *Science*, *59*(3), 513–520.

Walker, M. J. C., Berkelhammer, M., Björck, S., Cwynar, L. C., Fisher, D. A., Long, A. J., Lowe, J. J., Newnham, R. M., Rasmussen, S. O., & Weiss, H. (2012). Formal subdivision of the Holocene Series/Epoch: A Discussion Paper by a Working Group of INTIMATE (Integration of ice-core, marine and terrestrial records) and the Subcommission on Quaternary Stratigraphy (International Commission on Stratigraphy). *Journal of Quaternary Science*, *27*(7), 649–659. https://doi.org/10.1002/jqs.2565

Wang, Z., Fingas, M., & Page, D. S. (1999). Oil spill identification. *Journal of Chromatography A*, *843*(1–2), 369–411. https://doi.org/10.1016/S0021-9673(99)00120-X

Zanchetta, G., Van Welden, A., Baneschi, I., Drysdale, R., Sadori, L., Roberts, N., Giardini, M., Beck, C., Pascucci, V., & Sulpizio, R. (2012). Multiproxy record for the last 4500 years from Lake Shkodra (Albania/Montenegro). *Journal of Quaternary Science*, *27*(8), 780–789. https://doi.org/10.1002/jqs.2563

Zanetos, A., & Papathanassiou, E. (2005). *State of the Hellenic Marine Environment*. http://epublishing.ekt.gr/sites/ektpublishing/files/ebooks/Sohelme.pdf

Zervoudaki, S., Siokou, I., Krasakopoulou, E., Kontoyiannis, H., Pavlidou, A., Assimakopoulou, G., Katsiaras, N., Reizopoulou, S., Karageorgis, A. P., Kaberi, H., Lardi, P. I., Gerakaris, V., Tsiamis, K., Salomidi, M., Zeri, C., Pitta, E., Strogyloudi, E., Parinos, C., Hatzianestis, I., … Simboura, N. (2022). *Biogeochemical Characteristics in the Saronikos Gulf (Aegean Sea, Eastern Mediterranean)*. *2000*(June 2023), 2012–2015.

https://doi.org/10.1007/698_2022_898

Zheng, Y., Huang, Y., Andersen, R. A., & Amaral-Zettler, L. A. (2016). Excluding the di-unsaturated alkenone in the UK37 index strengthens temperature correlation for the common lacustrine and brackish-water haptophytes. *Geochimica et Cosmochimica Acta*, *175*, 36–46. https://doi.org/10.1016/j.gca.2015.11.024